ALMA MATER STUDIORUM · UNIVERSITÀ DI BOLOGNA

Scuola di Scienze
Dipartimento di Fisica e Astronomia
Corso di Laurea in Fisica

Stochastic effects in ultra slow-roll inflation

Relatore:
Dott. Francisco Pedro

Presentata da:
Mirko Longo

Anno Accademico 2017/2018

Abstract

In this work we apply the stochastic inflation formalism to backgrounds that deviate from standard slow-roll in a way that can lead to the production of primordial black holes. We analyse the effects of sudden transitions on the stochastic noise amplitude and its potential impact on the production of primordial black holes in single field inflation. We justify the claim that primordial black holes can be responsible for a significant fraction of the dark matter abundance today and estimate the required enhancement in the power spectrum. We introduce the Hamiltonian formalism and the coarse-graining of the quantum field and its momentum, allowing us to obtain a quantitative measure of the role of quantum diffusion in the production of primordial black holes. We mainly focus our analysis on a Starobinsky potential given that it is rich enough to allow for the dynamics of the scalar field during inflation to include an ultra slow-roll phase induced by a transition from a relatively large slow-roll parameter to a hierarchically smaller one. This has the effect of making the field perturbations undergo sudden transitions and rise from its ground state to an excited state.

We present two procedures that we employed when calculating the power spectrum: a numerical and an analytical one. Both methods show that stochastic effects are negligible at small scales where their amplitude is time dependent and vanishes at late times, and that for scales leaving the horizon after the ultra slow-roll phase the de Sitter estimate of $H^2/(4\pi^2)$ is approximately correct. We therefore demonstrate that the estimates in the literature are incomplete and that a revaluation of the role of stochastic effects on primordial black hole production is in order.

Sommario

In questo lavoro applicheremo il formalismo dell'inflazione stocastica a background che si discostano dallo slow-roll standard in un modo che puó portare alla produzione di buchi neri primordiali. Analizzeremo gli effetti di transizioni improvvise sull'ampiezza del rumore stocastico e il loro potenziale impatto nella produzione di buchi neri primordiali in modelli di inflazione con un singolo campo. Giustificheremo l'affermazione che i buchi neri primordiali possono essere responsabili di una frazione significativa dell'abbondanza della materia oscura oggi e stimeremo il necessario potenziamento nello spettro di potenza. Introdurremo il formalismo hamiltoniano e il 'coarse-graining' del campo quantistico e del suo momento, i quali ci permettono di ottenere una misura quantitativa del ruolo della diffusione quantistica nella produzione di buchi neri primordiali. Concentreremo principalmente la nostra analisi su un potenziale di tipo Starobinsky, dato che è abbastanza ricco da consentire alla dinamica del campo scalare durante l'inflazione di includere una fase di ultra slow-roll indotta da una transizione da un parametro relativamente grande ad uno gerarchicamente piú piccolo. Questo fa sì che le perturbazioni del campo subiscano improvvise transizioni e si elevino dal loro stato fondamentale a uno stato eccitato.

Presenteremo due procedure che abbiamo utilizzato per il calcolo dello spettro di potenza: una numerica e una analitica. Entrambi i metodi mostrano che gli effetti stocastici sono trascurabili a piccole scale, alle quali la loro ampiezza mostra una dipendenza dal tempo e si annulla a tempi elevati, e che per scale che lasciano l'orizzonte dopo la fase di ultra slow-roll la stima de Sitter di $H^2/(4\pi^2)$ è approssimativamente corretta. Dimostreremo quindi che le stime nella letteratura sono incomplete e che è necessaria una rivalutazione del ruolo degli effetti stocastici sulla produzione di buchi neri primordiali.

Contents

Chapter 1

An overview of modern cosmology

Cosmology [1, 2, 3] is possibly one of the oldest and most ambitious branches of science. Its quest is that of explaining the dynamics of the entire Universe. To complicate matters even further, cosmologists only have one sample since the Universe is, by definition, unique. We cannot observe a big number of Universes and formulate laws based on their statistical behaviour. This means that any theory we might articulate has to be tested on the very object we used to derive them in the first place. This is a very subtle point that leads any cosmological theory to be driven by observation rather than experimentation.

Given its nature, it is not unusual to make decisions in cosmology based on personal preference, cultural background or even aesthetics, which often guide its practitioners away from Nature's plan. We should therefore approach its study with an open mind.

The real turning point for cosmology was the 20th century when, in 1915, Einstein developed his theory of general relativity, which became the foundation of any modern cosmological theory. In an example of personal bias influencing the interpretation of a physical theory, Einstein later added in his equations a cosmological constant contribution in order to accommodate a static Universe, which was the main idea at the time. However in 1929, when Hubble measured the expansion of the Universe, he promptly discarded it, referring to it as his greatest blunder, although today the concept of a cosmological constant is reformulated as a possible dark energy contribution.

The definitive proof of the expansion of the Universe was the discovery of the cosmic microwave background radiation (CMB) in 1965, which many argue marked the beginning of modern cosmology. Although CMB shows the Universe was extremely homogeneous in the deep past/on large scales, today we observe huge jumps in density on galactic and smaller scales. These two very different behaviours are reconciled by combining observational CMB data with general relativity: in a mostly flat Universe and with the current observational constraints, we estimate an abundance of 68% dark energy [4] and 5% ordinary matter. The remaining 27% is a form of matter which solely interacts gravitationally, later dubbed dark matter. To this day, the debate on the nature of such a mysterious substance is still an open one.

One amongst the many possible candidates for (cold) dark matter is primordial black holes. These extremely small black holes are created at a very early stage in the evolution of the Universe and behave as pressureless dust afterwards. If they are produced in sufficient numbers they can account for a large fraction of dark matter.

The second concept in modern cosmology that is fundamental for our understanding of the Universe and its evolution is inflation, a period before the initial 'singularity' in the Hot Big Bang model in which the Universe underwent a phase of accelerated expansion. Such an unimaginably fast increase in size causes any inhomogeneity to be stretched out and washed away.

In this thesis we will connect the physics of inflation to that of dark matter through the study of formation of primordial black holes during inflation. This chapter will introduce the main ideas of modern cosmology and its many achievements, along with its limitations. We will discuss the problems that the vanilla Hot Big Bang model leaves unsolved, and the possible explanation that inflation gives for them.

1.1 First principles

Exactly like any other science, cosmology has a set of fundamental laws to draw upon when developing new theories. One of these is the cosmological principle. The name 'principle' stems from the fact that there was no data to support it when it was formulated in the early 20th century, but it was so fundamental and reasonable that it was hard to disprove it. Today, it serves as the starting point of all cosmology.

It describes a particular symmetry enjoyed by the Universe as a whole. It states that, on sufficiently large scales (beyond the large scale of galaxies), the Universe is both isotropic and homogeneous. This is a very strong assertion, as it links every patch of the Universe into a uniform structure.

One of the experimental confirmations of the cosmological principle is the high degree of homogeneity and isotropy found in the large scales of the cosmic microwave background. However, it is important to point out that this principle only applies to extremely large scales. Galactic scales definitely do not comply since, for instance, the Milky Way appears as a band across the sky, which clearly is neither homogeneous nor isotropic.

As we shall see in the following sections, the cosmological principle is strong enough to generate very simple but adequate models.

1.1.1 General relativity

The second fundamental idea every modern theory of the Universe is based on is Einstein's General Theory of Relativity. This theory of gravity is a natural generalisation of special relativity. Here we will briefly summarise some of its concepts.

The interval between two infinitesimally distanced events is given by

$$ds^2 = g_{\mu\nu} \, dx^\mu \, dx^\nu \,, \tag{1.1.1}$$

where repeated indices imply summation, μ and ν run from 0 to 3, $x^0 = ct$ is the time coordinate, x^i with $i = 1, 2, 3$ are space coordinates and the tensor $g_{\mu\nu}$ describes the geometry of space-time. Any particle moves in the background generated by $g_{\mu\nu}$ on a path γ such that

$$\delta \int_\gamma ds = 0. \tag{1.1.2}$$

From this equation, it can be shown that we obtain the equations of motion

$$\frac{d^2 x^\mu}{ds^2} + \Gamma^\mu_{\alpha\beta} \frac{dx^\alpha}{ds} \frac{dx^\beta}{ds}, \tag{1.1.3}$$

called a geodesic. Here, $\Gamma^\mu_{\alpha\beta}$ are the Christoffel symbols

$$\Gamma^\mu_{\alpha\beta} = \frac{1}{2} g^{\mu\lambda} \left(\frac{\partial g_{\lambda\alpha}}{\partial x^\beta} + \frac{\partial g_{\lambda\beta}}{\partial x^\alpha} - \frac{\partial g_{\alpha\beta}}{\partial x^\lambda} \right). \tag{1.1.4}$$

Equation (1.1.3) is extremely important, because it brings the idea that free particles move in a background determined by $g_{\mu\nu}$, which in turn is determined by the distribution of matter.

We can find generalised expression for the laws of conservation of energy and momentum. The energy-momentum tensor for a perfect fluid of pressure p and energy density ρ reads

$$T_{\mu\nu} = (p + \rho c^2) u_\mu u_\nu - p g_{\mu\nu}, \tag{1.1.5}$$

where u_μ is the 4-velocity

$$u_\mu = g_{\mu\alpha} \frac{dx^\alpha}{ds}. \tag{1.1.6}$$

The conservation law mentioned above is given by

$$T_\mu{}^\nu{}_{;\nu} = 0, \tag{1.1.7}$$

where ; indicates covariant derivation.

Einstein wanted to find a fundamental equation that involved the energy-momentum tensor $T_{\mu\nu}$ and the metric $g_{\mu\nu}$. This equation is given by

$$R_{\mu\nu} - \frac{1}{2} g_{\mu\nu} R = \frac{8\pi G}{c^4} T_{\mu\nu}, \tag{1.1.8}$$

where the tensor $R_{\mu\nu} = R^\alpha{}_{\mu\alpha\nu}$ can be obtained from the Riemann-Christoffel tensor

$$R^\alpha_{\beta\gamma\delta} = \frac{\partial \Gamma^\alpha_{\beta\delta}}{\partial x^\gamma} - \frac{\partial \Gamma^\alpha_{\beta\gamma}}{\partial x^\delta} + \Gamma^\alpha_{\kappa\gamma} \Gamma^\kappa_{\beta\delta} - \Gamma^\alpha_{\kappa\delta} \Gamma^\kappa_{\beta\gamma}, \tag{1.1.9}$$

$R = R^\alpha{}_\alpha$ is the Ricci scalar and $G_{\mu\nu} = R_{\mu\nu} - g_{\mu\nu} R/2$ is the Einstein tensor satisfying $G_\mu{}^\nu{}_{;\nu} = 0$.

8

1.1.2   The Friedmann-Robertson-Walker metric

Assuming that the cosmological principle holds, we need to find a metric which correctly reproduces a homogeneous and isotropic space-time. At large scales, the Universe can be treated as a continuous fluid. For now we choose as time variable the proper time t. In such general hypotheses, the metric of the Universe in polar coordinates (r, θ, φ) is given by

$$\mathrm{d}s^2 = c^2 \, \mathrm{d}t^2 - a(t)^2 \left(\frac{\mathrm{d}r^2}{1 - kr^2} + r^2 \, \mathrm{d}\Omega^2 \right), \tag{1.1.10}$$

where $a(t)$ is the scale factor, $\mathrm{d}\Omega^2 = \mathrm{d}\theta^2 + \sin^2\theta \, \mathrm{d}\varphi^2$ is the solid angle element and k is the curvature parameter. A metric such as (1.1.10) is called a Friedmann-Robertson-Walker (FRW) metric.

The curvature parameter k can take three different values. When $k = -1$ the geometry described by (1.1.10) is of the hyperbolic type, when $k = 0$ it is flat and when $k = 1$ it is spherical. The particular geometry of our Universe was long debated by cosmologists of the previous century. Einstein's equations and the cosmological principle are compatible with a spherical Universe, while observations preferred a flat one. Today, the idea of inflation strongly suggests an extremely flat Universe. This is because, as we will explain later, a sudden expansion tends to pull the geometry towards flatness.

1.1.3   The Hubble law

As we mentioned, the cosmological principle alone gives rise to many fundamental properties of our Universe. We already introduced the FRW metric. Let us now consider a triangle defined by three points O, O' and P, as depicted in figure 1.1. The velocity of P with respect to O' is given by

$$\vec{v}'(\vec{r}') = \vec{v}(\vec{r}) - \vec{v}(\vec{d}). \tag{1.1.11}$$

The homogeneity of the Universe as suggested by the cosmological principle forces the functions $\vec{v}$ and $\vec{v}'$ to be the same. Thus

$$\vec{v}(\vec{r} - \vec{d}) = \vec{v}(\vec{r}') = \vec{v}'(\vec{r}') = \vec{v}(\vec{r}) - \vec{v}(\vec{d}). \tag{1.1.12}$$

This implies that the relationship between the function $\vec{v}$ and its argument $\vec{r}$ is linear, meaning that there must be constants $H_i{}^j$ for $i, j = 1, 2, 3$ such that

$$v_i = H_i{}^j x_j. \tag{1.1.13}$$

If we now utilise the isotropy hypothesis in the cosmological principle, we can say that the velocity field $\vec{v}$ must be irrotational, i.e.

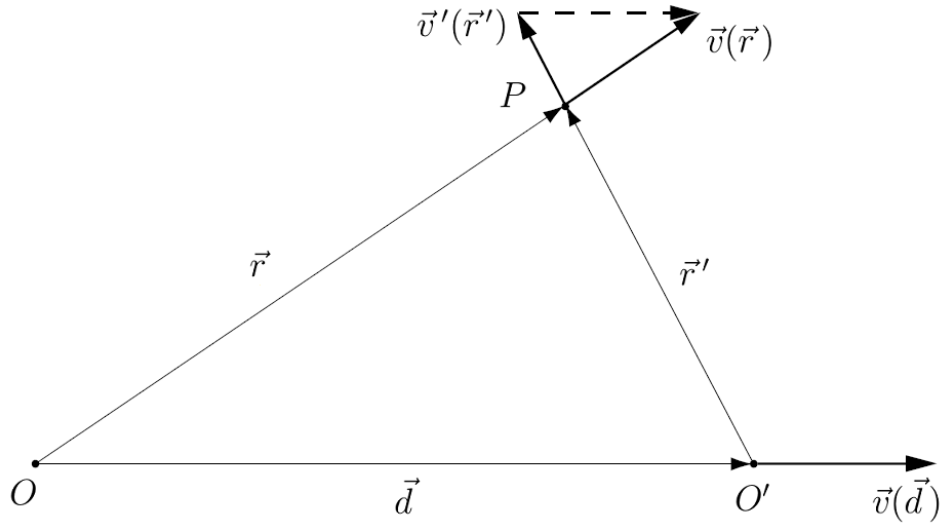$$\vec{\nabla} \times \vec{v} = \vec{0}. \tag{1.1.14}$$

Figure 1.1: Graphic representation of the Hubble law.

This means that the matrix formed by $H_i{}^j$ is symmetric and it can be diagonalised. Therefore

$$v_i = H x_i, \tag{1.1.15}$$

where H is a function of time only. Equation (1.1.15) is called the Hubble law. It can be shown using the FRW metric that

$$H(t) = \frac{\dot{a}}{a}, \tag{1.1.16}$$

where a dot represents derivation with respect to proper time t. This law implies that we can treat any spatial position as the origin of a coordinate system. The expansion of the Universe will look the same and will not depend neither on the position of the observer in the Universe nor the direction in which they point their instruments.

1.2 The Friedmann equations

We will make extensive use of the Friedmann equations throughout this work. In this section we will briefly sketch how to derive them starting from the basic ideas developed in section 1.1. They can be obtained from Einstein's field equations (1.1.8) assuming the Universe to be a perfect fluid whose energy-momentum tensor is given by (1.1.5) and whose metric is of the FRW type (1.1.10). The time-time component yields

$$\ddot{a} = -\frac{4\pi G}{3}\left(\rho + \frac{3p}{c^2}\right)a^2, \tag{1.2.1}$$

10

whereas the space-space component yields

$$a\ddot{a} + 2\dot{a}^2 + 2kc^2 = 4\pi G \left(\rho - \frac{p}{c^2}\right) a^2. \tag{1.2.2}$$

Using (1.2.1) to eliminate $\ddot{a}$ from (1.2.2) leads to

$$H^2 + \frac{kc^2}{a^2} = \frac{8\pi G}{3}\rho. \tag{1.2.3}$$

Equations (1.2.3) and (1.2.1) are called the Friedmann equations.

The Friedmann equations are not independent. Instead they are linked by the adiabatic expansion condition

$$\mathrm{d}(\rho c^2 a^3) = -p\,\mathrm{d}a^3 \tag{1.2.4}$$

(compare this equation with $\mathrm{d}E = -p\,\mathrm{d}V$).

Usually, we consider Universes whose state equation can be cast in the form

$$p = w\rho c^2, \tag{1.2.5}$$

where $0 \leq w \leq 1$. Notable examples of choice for the parameter w include the dust Universe ($w = 0$), the ultra-relativistic Universe ($w = 1/3$) and the stiff matter Universe ($w = 1$). We will not go over the evolution of said Universes. However, we will briefly mention a few general properties of Friedmannian Universes.

1.2.1 Friedmann models

From the Friedmann equations we can determine the time evolution of many quantities, such as the scale factor. It is useful to introduce the density parameter $\Omega = \rho/\rho_{\mathrm{c}}$, where

$$\rho_{\mathrm{c}} = \frac{3H^2}{8\pi G} \tag{1.2.6}$$

is the critical density. When evaluated at $a = a_0$ (the suffix 0 stands for any time $t = t_0$ we wish to calculate our expression at), the adiabatic condition (1.2.4) can be rewritten as

$$\left(\frac{\dot{a}}{a_0}\right)^2 - \frac{8\pi G\rho}{3}\left(\frac{a}{a_0}\right)^2 = H_0^2\left(1 - \Omega_0\right) = -\frac{kc^2}{a_0^2}. \tag{1.2.7}$$

From this expression we can find the physical interpretation of the density parameter Ω_0: when $k = -1, 0, 1$, we can see that $\Omega_0 < 1$, $\Omega_0 = 1$, $\Omega_0 > 1$ respectively. Thus, in order for the geometry of the Universe to be of the flat type, the energy density today ρ_0 must match precisely the critical density $\rho_{0,\mathrm{c}}$. Any slight variation would lead to a curved Universe. The flat scenario therefore seems impossible to achieve. Amongst all possible energy density, our Universe has to obtain one exact value. This is one of the

problems that the Hot Big Bang theory cannot explain by itself. We will later illustrate the solution widely accepted today by cosmologists, which is based on inflation.

Starting from (1.2.7), it can be shown that the time evolution of the density parameter Ω_w for a Universe dominated by energy with state equation $p = w\rho c^2$ at a time with scale factor a is given by

$$\Omega_w^{-1}(a) - 1 = \left(\frac{a}{a_0}\right)^{1+3w} \left(\Omega_{0,w}^{-1} - 1\right). \tag{1.2.8}$$

This expression will be analysed further in section 1.3.3 when we discuss the flatness problem.

1.2.2 The particle horizon

Consider the set of points which could potentially be in causal connection with an observer at time t. Let us place the observer at the origin of a coordinate system. Since information does not travel faster than light, this set is clearly finite if t is finite. It is made up of all the light signals that reached the observer before t and therefore were emitted at a time t' such that $0 < t' < t$. Such a point has to be contained in a sphere centred at the origin of the coordinate system and whose radius is given by

$$R_H(t) = a(t) \int_0^t \frac{c\,dt'}{a(t')}, \tag{1.2.9}$$

called the particle horizon at time t. Any light signal coming from a point distant $d > R_H(t)$ cannot influence the observer before t. The integral in (1.2.9) can be easily solved if we approximate $\Omega_w \simeq 1$ during early times. We obtain

$$R_H(t) \simeq \frac{2c}{H_0 \Omega_{0,w}^{1/2}(3w+1)} \left(\frac{a}{a_0}\right)^{3(1+w)/2}, \tag{1.2.10}$$

which, if we turn to proper time, becomes

$$R_H(t) \simeq \frac{3(1+w)}{1+3w} ct. \tag{1.2.11}$$

1.3 The Hot Big Bang theory and its problems

Running the time evolution of the scale factor backwards through (1.2.7) we can see that, for any value of Ω, the function $a(t)$ is monotonous. Thus there must have been a moment in time when $a = 0$, which means that all matter in the entire Universe must have been compressed into a singularity. This is unavoidable in all models where $-1/3 < w \leq 1$.

There is no reason to believe that general relativity still holds in such extreme densities and temperatures. Therefore, if we want to fully describe the earliest moments in the life of our Universe we have to develop new physics. Quantum gravity is still very much in its infancy, and we are far from a unified theory of everything. However, we can safely assume that the singularity is only a sign of the incompleteness of modern cosmology, rather than a true physical phenomenon.

There are some tricks that we can employ if we want to circumvent the singularity. Firstly, it is possible to generalise the condition $-1/3 < w \leq 1$ to include Universes in which the parameter w lies in the range $-1 \leq w \leq -1/3$. If we look at the Friedmann equation (1.2.1) it can be seen that, in such a situation, we can have $\ddot{a} > 0$. This means that the monotony of $a(t)$ is broken and the singularity is avoided. Fluids which do not satisfy $-1/3 < w \leq 1$ are said to violate strong energy condition. An example of this behaviour can be found if one adds a cosmological constant $\Lambda > 0$ to Einstein's equations (1.1.8):

$$R_{\mu\nu} - \frac{1}{2}g_{\mu\nu}R = \frac{8\pi G}{c^4}T_{\mu\nu} + g_{\mu\nu}\Lambda. \tag{1.3.1}$$

The effects of a term similar to this supposedly dominated the dynamics in the very early stages of the Universe. Its accepted physical interpretation today is that it is a quantity related to the vacuum energy density of a scalar field.

1.3.1 The monopole problem

Generally speaking, 'hot' Big Bang models predict that the temperature increases as we go back in time. Various high energy extensions of known physics predict the existence of topological defects. The types of defects in the theory are categorised by their dimensionality: there are magnetic monopoles (zero-dimensional), cosmic strings (one-dimensional), domain walls (two-dimensional) and finally textures (three-dimensional).

Defects are predicted to be created in great number in the early Universe. However not a single piece of evidence of their existence has been collected yet. In this section we shall discuss why monopoles should be abundant.

It can be shown that we expect a density parameter for magnetic monopoles today

$$\Omega_{0,\mathrm{MM}} > \frac{m_{\mathrm{MM}}}{m_{\mathrm{p}}}\Omega_{\mathrm{b}} \simeq 10^{16}, \tag{1.3.2}$$

which is absurdly large. As we shall see, inflation gives a very elegant solution to this problem.

We also point out that domain walls and cosmic strings should be very abundant as well. This claim can be verified through a discussion similar to the above.

1.3.2 The horizon problem

In section 1.2.2 we introduced the idea of a particle horizon, which is ultimately caused by the finiteness of the speed at which information travels. This means that there is no reason to expect that large patches of the Universe be in causal connection unless they are contained inside each others particle horizons. Consider for instance the CMB. The time of last scattering $t_{ls} \simeq 350$ kyrs represents the time beyond which the Universe stopped being opaque. The maximum distance between two particles in causal connection at CMB time is then given by

$$R_{ls} \simeq \frac{c(t_0 - t_{ls})}{1 + z_{ls}} \simeq \frac{ct_0}{z_{ls}}, \tag{1.3.3}$$

where $z_{ls} \simeq 1000$ is the redshift of last scattering. Since at that epoch the Universe was already dominated by matter ($w = 0$), the particle horizon is

$$R_H(t_{ls}) \simeq 3ct_0 z_{ls}^{-3/2} \simeq \frac{R_{ls}}{10}. \tag{1.3.4}$$

This is not possible, since $R_H(t_{ls}) < R_{ls}$ would mean that two patches of the Universe were in causal connection beyond their particle horizons!

Many solutions were proposed but ultimately, this problem was definitively solved by an inflationary solution, as we will show in section 1.4.

1.3.3 The flatness problem

As we mentioned, the Friedmann Universe has three possible geometries: closed, open or flat. From the Friedmann equations, one can derive the time evolution of temperature in these three cases.

When the Universe is closed, it undergoes a period of expansion in which a maximum value for the scale factor is achieved, then it rapidly collapses reaching a singularity again after about $t_{Pl} \simeq 10^{-43}$ s.

If instead we assume an open geometry, it can be shown that today's temperature $T_0 \simeq 3$ K would have been reached after

$$t_0 \simeq t_{Pl} \frac{T_{Pl}}{T_0} \simeq 10^{-11} \text{ s.} \tag{1.3.5}$$

This value is unrealistic since we know our Universe is about 10^{10} yrs old. This is referred to as the age problem, since there is apparently no explanation as to why the Universe managed lo last this long.

Another way to phrase this is by analysing the density parameter of such a long-lasting Universe. Since neither closed nor open geometry yield realistic results, our Universe must be of the flat type. However, as we stressed before, flat Universes require

severe fine-tuning since the energy density today ρ_0 must be very close the critical density today $\rho_{0,\text{c}} = 3H_0^2/(8\pi G)$. From (1.2.8), it can be shown that

$$\Omega(t_{\text{Pl}}) \simeq 1 + (\Omega_0 - 1)10^{-60}, \tag{1.3.6}$$

meaning that the density parameter at Planck time must have been equal to 1 within at least 60 digit precision! This is the flatness problem, the question of how the Universe was so flat.

1.4   The inflationary paradigm

Most (but not all) problems of the Hot Big Bang model can be solved by assuming that the Universe underwent a period of accelerated expansion before the Big Bang itself [5]. Such a phase would elegantly solve the flatness and horizon problems, while it could also provide a possible explanation for the lack of defects observed today, since they would be diluted during the expansion as long as they are created before inflation. Any fluctuation in the background gravitational field and energy density is suppressed because of the stretching of space-time due to the exponentially accelerated expansion. The smoking gun of this mechanism is represented by the extreme homogeneity observed in the cosmic microwave background radiation, whose tiny anisotropies would then go on to form the large scale structure of our Universe.

This feature of inflation is extremely appealing from a theoretical point of view because of its strong independence on initial conditions. Indeed, inflation predicts there must be a phase, called slow-roll, in which the motion of the field driving inflation is mostly dominated by a friction term. This means that the field is 'slowly rolling' towards the minimum of the potential. If one plots the phase-space of the inflaton during inflation, one clearly sees that slow-roll is a dynamical attractor, meaning that for a huge range of initial conditions (i.e. values of the inflaton field and its velocity at the beginning of observable inflation) the motion is inevitably attracted towards this slow-roll phase. We will expand more on slow-roll in the next chapter.

How can such a phase be achieved? In this section we will work in natural units, i.e. we take $\hbar = c = 1$. During inflation, the energy density of vacuum dominates over all other forms of energy, meaning $\rho_\Lambda \simeq V(\phi)$, where ϕ is the field driving inflation. When $V \simeq \text{const.}$, the expansion is exponential $a \propto e^t$.

The term 'inflation' is generic: in practice, there are many ways in which one can achieve an accelerated expansion. Historically, the first person to formulate such a phase was Guth [6] in 1981 with old inflation, then Linde proposed an updated model later dubbed new inflation. There are many more models that have been developed by cosmologists over the years. In what follows we are interested in the main features of the inflationary framework rather than in particular models.

The inflaton's dynamics is determined by the classical Lagrangian density

$$\mathcal{L}_\phi = \frac{1}{2}\dot{\phi}^2 - V(\phi). \tag{1.4.1}$$

The field ϕ has an effective energy density ρ_ϕ and an effective pressure p_ϕ given by

$$\rho_\phi = \frac{1}{2}\dot{\phi}^2 + V(\phi), \tag{1.4.2}$$

$$p_\phi = \frac{1}{2}\dot{\phi}^2 - V(\phi). \tag{1.4.3}$$

The time evolution of the field ϕ can be obtained as the Euler-Lagrange equation of the Lagrangian density (1.4.1), which in cosmic time reads

$$\frac{\mathrm{d}}{\mathrm{d}t}\frac{\partial(\mathcal{L}_\phi a^3)}{\partial\dot{\phi}} - \frac{\partial(\mathcal{L}_\phi a^3)}{\partial\phi} = 0. \tag{1.4.4}$$

Recall that $\mathcal{L}_\phi a^3$ is the true Lagrangian. Using (1.4.1) yields

$$\ddot{\phi} + 3\frac{\dot{a}}{a}\dot{\phi} + \frac{\partial V(\phi)}{\partial\phi} = 0. \tag{1.4.5}$$

This equation describes the motion of the field ϕ while it rolls towards its minimum. When the field is in the slow-roll phase of inflation, we can approximate the Friedmann equation (1.2.3) by imposing $k = 0$, because the fast expansion causes ρ_ϕ to dominate over ρ and kc^2/a^2, meaning that

$$\left(\frac{\dot{a}}{a}\right)^2 \simeq \frac{8\pi G}{3}\rho_\phi \simeq \frac{8\pi G}{3}V(\phi), \tag{1.4.6}$$

using $\dot{\phi}^2/2 \ll V(\phi)$ during slow-roll. Equation (1.4.6) has the de Sitter solution

$$a \propto \exp\left(\frac{t}{\tau}\right), \tag{1.4.7}$$

where

$$\tau = \left[\frac{3}{8\pi G V(\phi)}\right]^{1/2}. \tag{1.4.8}$$

Using typical values for $V(\phi)$, we get $\tau \simeq 10^{-34}$ s. This gives us an idea of the characteristic time scales of inflation. As we will justify later, in order for inflation to solve the Big Bang problems, there must be an expansion of about e^{70}. This means that the scale factor a (which essentially measures how big the Universe is) during inflation increases of about 30 orders of magnitude in only 10^{-34} s! This explains why homogeneity is achieved regardless of the initial state.
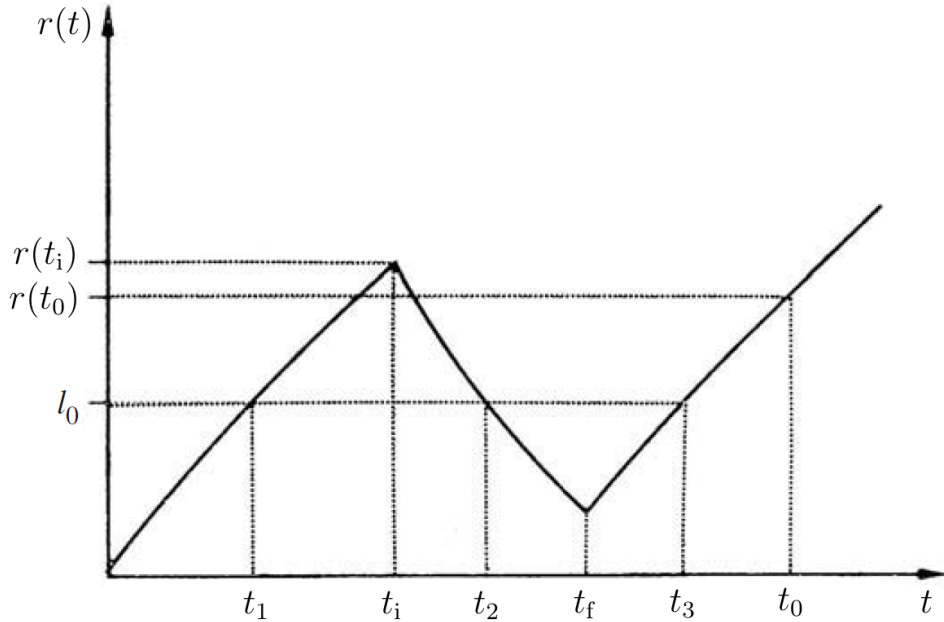
16

Figure 1.2: The inflationary solution to the horizon problem. Taken from [1]

1.4.1 Inflationary solution to the horizon problem

Let us now discuss how inflation solves the horizon problem. Consider a scale L. It can enter causal connection only after a time t_L has passed since the singularity such that $R_H(t_L) = L$. It is convenient to work with the Hubble sphere $R(t) = c/H$ rather the particle horizon $R_H(t)$. There is a subtle difference in the definition of the two quantities, but they are about equal during early times, so we will refer to one or the other indistinctly. In addition, we will work with comoving quantities, therefore we need the comoving particle horizon

$$r = R\frac{a_0}{a} = \frac{ca_0}{\dot{a}}. \tag{1.4.9}$$

This quantity always increases in non-inflation times, since $\dot{a}$ is a monotonous decreasing function. This means that more and more points enter causal connection as time passes.

Imagine now that there is a period between t_i and t_f where a comoving scale l_0 escapes the horizon $r(t)$. We stress that escaping this horizon does not violate causality in any way. After all, we are talking about comoving scales, so really what is happening here is that the points in space are moving apart faster than the speed of light due to the sudden expansion, and it does not imply superluminal speed for any physical object.

The scale l_0 can escape the horizon if $l_0 > r(t)$. In order for $r(t) \propto \dot{a}^{-1}$ to decrease, we must have an accelerated expansion $\ddot{a} > 0$. After t_f, the usual decelerated expansion is restored. We depicted in figure 1.2 the behaviour of $r(t)$. This picture allows us to understand why CMB scales appear to be in causal connection. Imagine that l_0 is such

a scale. It enters the horizon at t_1, before inflation. Between t_1 and t_2 this scale has plenty of time to reach homogeneity. An observer at t_3 however would be surprised to see that the scale l_0 is already in causal connection, provided he does not know of inflation. He would think l_0 should be inhomogeneous because it is the first time it enters causal connection.

Therefore, the horizon problem is solved if

$$r(t_0) \leq r(t_i). \tag{1.4.10}$$

This condition can be ultimately used to impose a lower limit on the duration of inflation. Indeed, if the beginning of inflation t_i were too close to its end t_f, the scale l_0 from figure 1.2 would have no time to move out of the comoving horizon. In order to find this condition, let us divide the age of the Universe in three intervals: (t_i, t_f), (t_f, t_{eq}) and (t_{eq}, t_0), where t_{eq} is the equivalence time, the moment in which the radiation and matter density parameters where equal. Let us call $w_{i,j}$ the constant in the state equation between two phases i and j. Another way we can write (1.2.7) is

$$\left(\frac{\dot{a}}{a_0} \right)^2 = H_0^2 \left[\Omega_{0,w_{i,j}} \left(\frac{a_0}{a} \right)^{1+3w_{i,j}} + \left(1 - \Omega_{0,w_{i,j}} \right) \right]. \tag{1.4.11}$$

From this equation, assuming $\Omega_{i,j} \simeq 1$, we get

$$\frac{H_i a_i}{H_j a_j} \simeq \left(\frac{a_i}{a_j} \right)^{-(1+3w_{i,j})/2}. \tag{1.4.12}$$

Let us set $w_{i,f} = w < -1/3$, $w_{f,eq} = 1/3$ and $w_{eq,0} = 0$. The requirement that inflation lasts long enough for the Big Bang problems to be solved reads

$$r(t_i) = \frac{ca_0}{\dot{a}_i} > r(t_0) = \frac{c}{H_0}. \tag{1.4.13}$$

Using (1.4.12) twice to link the three phases together we obtain

$$\left(\frac{a_f}{a_i} \right)^{-(1+3w)} > 10^{60} z_{eq}^{-1} \left(\frac{T_f}{T_{Pl}} \right)^2. \tag{1.4.14}$$

Therefore the number of e-foldings $N_e = \ln(a_f/a_i)$ of inflation should be

$$N_e > 60 \left[\frac{2.3 + \frac{1}{30} \ln(T_f/T_{Pl}) - \frac{1}{60} \ln z_{eq}}{|1 + 3w|} \right] \simeq 60. \tag{1.4.15}$$
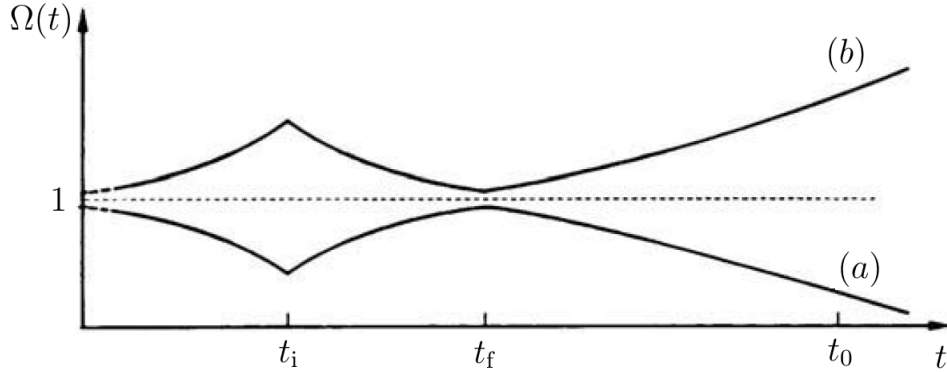
Figure 1.3: Inflationary solution to the flatness problem. When $t_i < t < t_f$ the accelerated expansion drives the evolution parameter $\Omega(t)$ towards 1. Then it diverges again, but if inflation lasts long enough, the divergence is very small and delayed until much later than t_0. Taken from [1]

1.4.2 Inflationary solution to the flatness problem

Let us consider (1.2.8). It can be cast in the form

$$(\Omega^{-1} - 1)\rho a^2 = (\Omega_0^{-1} - 1)\rho_0 a_0^2. \tag{1.4.16}$$

Dividing the history of the Universe in the three intervals (t_i, t_f), (t_f, t_{eq}) and (t_{eq}, t_0) in the same manner as section 1.4.1, we obtain with some manipulation

$$\left(\frac{a_f}{a_i}\right)^{-(1+3w)} = \frac{1 - \Omega_i^{-1}}{1 - \Omega_0^{-1}} 10^{60} z_{eq}^{-1} \left(\frac{T_f}{T_{Pl}}\right)^2. \tag{1.4.17}$$

It can be shown that the flatness problem is solved when the density parameter Ω_i at the beginning of inflation is closer to unity than today or, in other words, when

$$\frac{1 - \Omega_i^{-1}}{1 - \Omega_0^{-1}} \geq 1. \tag{1.4.18}$$

This condition leads to an expression similar to (1.4.15), meaning that the requirement inflation solves the Hot Big Bang problems is that $N_e > 60$.

Chapter 2

Stochastic inflation

In chapter 1 we motivated the need for a phase of accelerated expansion at times before the usual Big Bang theory, mainly motivated by the search of a solution to the flatness and horizon problems. Inflation is a very promising idea, since it also gives an explanation to other problems (such as the monopole problem) and provides the seeds for structure formation.

In this chapter we will introduce the main formalism of slow-roll and ultra slow-roll (USR) during inflation. Slow-roll is achieved when the kinetic term is small when compared to the potential term, whereas during ultra slow-roll the potential becomes extremely flat so that acceleration is no longer negligible. The first ideas of slow-roll inflation were introduced around 1982 by Linde [7], Albrecht and Steinhardt [8], Starobinsky [9] and it is able to solve the usual Hot Big Bang problems and explain the CMB spectrum.

In this chapter we will introduce the PBH formation mechanism in section 2.1 that leads us to the study of stochastic effects during inflation. Then we will develop the main formalism of stochastic inflation in section 2.2, following the discussion of [10]. We will then present the different approaches to the problem of stochastic effects in PBH production. We will report the main results of [11] in section 2.3.1, of [12] in section 2.3.2 and of [13] in section 2.3.3. Finally, we will comment on them in section 2.3.4.

2.1   Primordial black holes

PBHs are created in the early Universe and can make up between 10% and 100% of the total dark matter abundance according to the latest observational constraints. The allowed mass range lies around $10^{-17} M_\odot$ and $10^{-14} M_\odot$, with an extra open window around $10^{-12} M_\odot$. These masses are extremely tiny when compared to the masses of astrophysical black holes, which are typically between $10^2 M_\odot$ and $10^9 M_\odot$, and correspond to atomic size black holes. The mechanism to generate PBHs which will be analysed

throughout this article is the amplification of the density perturbations during inflation.

Amplification has to be strong enough and take place at the correct scales to generate PBHs while being insignificant enough at cosmological background (CMB) scales not to interfere with CMB observations. However, it cannot be arbitrarily big, since it has to be small enough for perturbation theory to still hold. We will employ a single field inflationary model, which is the simplest and most natural model. The PBH formation is thought to happen during an ultra slow-roll regime placed in between two slow-roll phases. This particular structure is extremely difficult to find through a top-down approach: the potential of the single field needs to be rich enough to allow for PBH formation. However, there are many examples of simple potentials which manage to reproduce most of the features that the power spectrum should have in order to seed PBH formation. A detailed description of the potentials utilised in this work is given in section 3.1.

The fraction of the total energy density of PBHs with mass M at PBH formation (denoted by f) is given by [14, 15]

$$\beta_{\mathrm{f}}(M) = \left.\frac{\rho_{\mathrm{PBH}}(M)}{\rho_{\mathrm{tot}}}\right|_{\mathrm{f}}. \tag{2.1.1}$$

We shall neglect any non-Gaussianity effects in the curvature perturbation distribution. Therefore they are described by Gaussian statistics with width $\sigma_M = \sigma(M)$. Let us assume there exists a critical value ζ_{c} for PBH formation: any energy density higher than this value will collapse into a primordial black hole after its respective scale re-enters the horizon. Therefore, the probability of large fluctuations collapsing is given by

$$\beta_{\mathrm{f}}(M) = \int_{\zeta_{\mathrm{c}}}^{\infty} \frac{1}{\sqrt{2\pi}\sigma_M} e^{-\frac{\zeta^2}{2\sigma_M^2}} \, \mathrm{d}\zeta. \tag{2.1.2}$$

The critical value ζ_{c} is usually taken to be close to unity. It can be shown that $\sigma_M \ll \zeta_{\mathrm{c}}$. This amounts to stating that the Gaussian distribution describing curvature perturbations is extremely peaked. With this approximation, we can write the PBH density as

$$\beta_{\mathrm{f}}(M) \simeq \frac{\sigma_M}{\sqrt{2\pi}\zeta_{\mathrm{c}}} e^{-\frac{\zeta_{\mathrm{c}}^2}{2\sigma_M^2}}. \tag{2.1.3}$$

The horizon mass is the mass of the black hole according to an observer sitting just outside the event horizon. At the classical level, it can be interpreted as the mass that can never escape the black hole's event horizon. It is defined as

$$M = \left.\frac{4\pi\rho_{\mathrm{tot}}}{3H^3}\right|_{\mathrm{f}} = \frac{1}{2GH_{\mathrm{f}}}, \tag{2.1.4}$$

where f indicates that the quantity needs to be evaluated at horizon re-entry. The last step was achieved through Friedmann equation (1.2.3).

We assume that the mass of primordial black holes is proportional to its horizon mass (2.1.4), so that their mass is [16]

$$M_{\text{PBH}} = \frac{\gamma}{2GH_{\text{f}}},$$ (2.1.5)

where the constant γ depends on the efficiency of the gravitational collapse (typically $\gamma \simeq 0.5$). Now, since primordial black holes are assumed to be dark matter, it is reasonable that the PBH density ρ_{PBH} behaves as matter ($w = 0$), therefore its evolution looks like $\rho_{\text{PBH}} = \rho_{\text{PBH}}^0 (a_0/a)^3$. Thus

$$\begin{aligned}
\beta_{\text{f}}(M) &= \frac{\rho_{\text{PBH}}(M)\big|_{\text{f}}}{\rho_{\text{tot}}\big|_{\text{f}}} = \frac{\rho_{0,\text{PBH}}(M)}{\rho_{\text{tot}}\big|_{\text{f}}} \left(\frac{a_0}{a_{\text{f}}}\right)^3 \\
&= \frac{\rho_{0,\text{PBH}}(M)}{\rho_{0,\text{DM}}} \left(\frac{a_0}{a_{\text{f}}}\right)^3 \frac{\rho_{0,\text{DM}}}{\rho_{\text{tot}}\big|_{\text{f}}},
\end{aligned}$$ (2.1.6)

where a_{f} is the scale factor evaluated at formation time. Let us name $f_{\text{PBH}}(M) = \rho_{0,\text{PBH}}(M)/\rho_{0,\text{DM}}$ the fraction of the total dark matter energy density in PBHs with mass M today. For simplicity, we can shift the scale factor so that today $a_0 = 1$. Additionally, the total energy density ρ_{tot} time evolution for a mostly flat Universe can be expressed in terms of the critical energy density today $\rho_{0,\text{c}} = 3H_0^2/(8\pi G)$ as

$$\rho_{\text{tot}} = \rho_{0,\text{c}} \left(\frac{H}{H_0}\right)^2.$$ (2.1.7)

These considerations allow us to write the fraction of the total energy density of PBHs with mass M at PBH formation as

$$\begin{aligned}
\beta_{\text{f}}(M) &= f_{\text{PBH}}(M) \left(\frac{1}{a_{\text{f}}}\right)^3 \frac{\rho_{0,\text{DM}}}{\rho_{0,\text{c}}} \frac{\rho_{0,\text{c}}}{\rho_{\text{tot}}\big|_{\text{f}}} \\
&= f_{\text{PBH}}(M) \frac{\Omega_{0,\text{DM}}}{a_{\text{f}}^3} \left(\frac{H_0}{H_{\text{f}}}\right)^2.
\end{aligned}$$ (2.1.8)

Using current constraints on cosmological parameters and setting $f_{\text{PBH}}(M) \simeq 1$, it can be shown that (2.1.8) leads to

$$\beta_{\text{f}}(M) \simeq 10^{-8} \sqrt{\frac{M}{M_\odot}}.$$ (2.1.9)

If we consider a mass distribution sharply peaked at $M = 10^{-15} M_\odot$ we find $\beta_{\text{f}}(M) \simeq 3 \times 10^{-16}$. Comparing this result to (2.1.3) for $\zeta_{\text{c}} = 1$ shows $\sigma_M \simeq 0.12$. Recalling that the power spectrum is proportional to σ_M^2 and that at CMB scales the scalar power spectrum

is $\mathcal{O}(10^{-9})$, this means that an enhancement of about 7 orders of magnitude must be achieved in order to comply with current observational constraints. This enhancement can indeed be achieved in the framework of single field inflation by inducing an extremely flat region in the scalar potential. This leads to an ultra slow-roll phase that must last long enough for its effects to be meaningful.

2.2 Coarse-graining in stochastic inflation

In standard inflation, the background expands in a homogeneous and isotropic manner, with negligible back-reaction. In the following sections we will analyse what happens if we introduce quantum perturbations in this background. These scalar perturbations undergo a quantum-to-classical transition, meaning on super-Hubble scales they can be treated as classical fields. This behaviour is well treated in a stochastic formalism, which effectively separates the field in its long-wavelength and small-wavelength parts, each obeying different sets of equations. The scale where the quantum-to-classical transition is achieved has to be chosen arbitrarily by selecting a cut-off wavelength. The quantum part of the field and its momentum start playing a significant role above this wavelength. This procedure is often referred to as the 'coarse-graining' of the inflaton.

The purpose of this chapter is to study these quantum fluctuations in a stochastic formalism, and to understand to which extent these modify the dynamics of the classical coarse-grained field. If significant enough, they might cause the inflaton to deviate from its regular slow-roll dynamics.

Deviations from the classical background trajectory can be extremely important when calculating PBH abundance, since they affect it exponentially, as per (2.1.3).

2.2.1 Stochastic inflation in the Hamiltonian formalism

In slow-roll, the Hubble factor $H = \dot{a}/a$ is almost constant. This can be expressed by requiring that the Hubble parameters

$$\epsilon_{n+1} = \frac{\mathrm{d}\ln|\epsilon_n|}{\mathrm{d}N_e} \tag{2.2.1}$$

are small. We can set $\epsilon_0 = H_{\mathrm{in}}/H$. The slow-roll condition is then

$$|\epsilon_n| \ll 1, \tag{2.2.2}$$

for all $n > 0$. Alternatively, the Hubble slow-roll parameters ϵ_i are usually renamed as follows: $\epsilon_1 = \epsilon$, $\epsilon_2 = \eta$ and finally $\epsilon_3 = \kappa$.

The dynamics of a scalar field ϕ minimally coupled to gravity in a 4-dimensional curved space-time with metric $g_{\mu\nu}$ is described by the action

$$S = \int \mathrm{d}^4x \sqrt{-g} \left[\frac{M_{\mathrm{Pl}}^2}{2} R - \frac{1}{2} g^{\mu\nu} \partial_\mu\phi \partial_\nu\phi - V(\phi) \right]. \tag{2.2.3}$$

Here R is the scalar curvature and $V(\phi)$ is the potential of the scalar field. The Hamiltonian formulation is obtained by foliating 4-dimensional space-time into a set of 3-dimensional space-like hyper-surfaces. The foliation is determined by the lapse function $N(\tau, x^i)$ and the shift vector $N^i(\tau, x^i)$. The line element is then given by

$$ds^2 = -N^2 d\tau^2 + \gamma_{ij}(N^i d\tau + dx^i)(N^j d\tau + dx^j), \tag{2.2.4}$$

where γ_{ij} is the induced metric on the 3-dimensional space-like hyper-surfaces.

The scalar sector has canonical variables ϕ and $\pi_\phi = \delta S/\delta\dot{\phi}$ with Poisson brackets $\{\phi(\vec{x}), \pi_\phi(\vec{y})\} = \delta^{(3)}(\vec{x}-\vec{y})$. Similarly, for the gravitational sector, the canonical variables are γ_{ij} and $\pi^{ij} = \delta S/\delta\dot{\gamma}_{ij}$ with Poisson brackets $\{\gamma_{ij}(\vec{x}), \pi^{kl}(\vec{y})\} = (\delta_i^k \delta_j^l + \delta_i^l \delta_j^k)\delta^{(3)}(\vec{x}-\vec{y})/2$.

The total Hamiltonian reads

$$C = \int d^3x \left[N(\mathcal{C}^{\mathrm{G}} + \mathcal{C}^\phi) + N^i(\mathcal{C}_i^{\mathrm{G}} + \mathcal{C}_i^\phi) \right]. \tag{2.2.5}$$

Here ϕ and G stand for the scalar and the gravitational sectors respectively. $\mathcal{C} = \mathcal{C}^{\mathrm{G}} + \mathcal{C}^\phi$ and $\mathcal{C}_i = \mathcal{C}_i^{\mathrm{G}} + \mathcal{C}_i^\phi$ are the scalar and the gravitational constraint respectively. The scalar constraints read

$$\begin{aligned}
\mathcal{C}^\phi &= \frac{1}{2\sqrt{\gamma}}\pi_\phi^2 + \frac{\sqrt{\gamma}}{2}\gamma^{ij}\partial_i\phi\partial_j\phi + \sqrt{\gamma}V(\phi), \\
\mathcal{C}_i^\phi &= \pi_\phi\partial_i\phi,
\end{aligned} \tag{2.2.6}$$

where γ denotes the determinant of γ_{ij}. The constraints in the gravitational sector have similar forms.

The time evolution of any function F of the phase-space variables is given by

$$\dot{F}(\gamma_{ij}, \pi^{kl}, \phi, \pi_\phi) = \{F, C\}. \tag{2.2.7}$$

The Hamilton equations $\dot{\phi} = \{\phi, C\}$ and $\dot{\pi}_\phi = \{\pi_\phi, C\}$ then read

$$\dot{\phi}(\vec{x}) = \int d^3y \left[N(\vec{y})\{\phi(\vec{x}), \mathcal{C}^\phi(\vec{y})\} + N^i(\vec{y})\{\phi(\vec{x}), \mathcal{C}_i^\phi(\vec{y})\} \right], \tag{2.2.8}$$

$$\dot{\pi}_\phi(\vec{x}) = \int d^3y \left[N(\vec{y})\{\pi_\phi(\vec{x}), \mathcal{C}^\phi(\vec{y})\} + N^i(\vec{y})\{\pi_\phi(\vec{x}), \mathcal{C}_i^\phi(\vec{y})\} \right]. \tag{2.2.9}$$

Using (2.2.6) allows us to find

$$\dot{\phi} = \frac{N}{\sqrt{\gamma}}\pi_\phi + N^i\partial_i\phi, \tag{2.2.10}$$

$$\dot{\pi}_\phi = -N\sqrt{\gamma}V_{,\phi} + \partial_i(N\sqrt{\gamma}\gamma^{ij}\partial_j\phi) + N^i\partial_i\pi_\phi + \pi_\phi\partial_i N^i, \tag{2.2.11}$$

where $V_{,\phi} = \partial V / \partial \phi$.

Let us now assume that ϕ is sufficiently decoupled from the metric that perturbations can be ignored (we will work out the coupled case in appendix A). In flat space-time, the line element (2.2.4) then simply becomes

$$\mathrm{d}s^2 = -N(\tau)^2 \mathrm{d}\tau^2 + a^2 \delta_{ij} \mathrm{d}x^i \mathrm{d}x^j. \qquad (2.2.12)$$

Notice the lapse function only depends on time and the shift vector is null. Choosing a lapse function amounts to choosing a clock. Indeed, $N = 1$ corresponds to working with cosmic time, $N = a$ with conformal time and $N = 1/H$ with number of e-folds. The metric reads $\gamma_{ij} = p\delta_{ij}$. This gives rise to a particularly simple expression for the Hamilton equations (2.2.10) and (2.2.11), which now become

$$\dot{\phi} = \frac{N}{a^3} \pi_\phi, \qquad (2.2.13)$$

$$\dot{\pi}_\phi = -Na^3 V_{,\phi} + Na\Delta\phi, \qquad (2.2.14)$$

where $\Delta = \delta^{ij} \partial_i \partial_j$ is the 3-dimensional Laplace operator.

2.2.2 Langevin equation in phase space

In order to study the stochastic behaviour of the inflaton it is necessary to split the scalar field ϕ into its small and long wavelength parts. This is achieved through the introduction of a cut-off wavelength in Fourier space

$$k_\sigma = \sigma aH, \qquad (2.2.15)$$

where σ is the ratio between the Hubble radius and the cut-off wavelength. It can be thought of as a time variable. Its effects disappear from all physical quantities in the limit $\sigma \ll 1$. The expansion of some physical quantities about this limit will be investigated further in 2.2.4.

The cut-off allows us to decompose the scalar field as $\phi = \bar{\phi} + \phi_Q$ and its momentum as $\pi_\phi = \bar{\pi} + \pi_Q$, where

$$\phi_Q = \int_{\mathbb{R}^3} \frac{\mathrm{d}^3 k}{(2\pi)^{3/2}} W\left(\frac{k}{k_\sigma}\right) \left[a_{\vec{k}} \phi_{\vec{k}}(\tau) e^{-i\vec{k}\cdot\vec{x}} + a_{\vec{k}}^\dagger \phi_{\vec{k}}^\star(\tau) e^{i\vec{k}\cdot\vec{x}}\right], \qquad (2.2.16)$$

$$\pi_Q = \int_{\mathbb{R}^3} \frac{\mathrm{d}^3 k}{(2\pi)^{3/2}} W\left(\frac{k}{k_\sigma}\right) \left[a_{\vec{k}} \pi_{\vec{k}}(\tau) e^{-i\vec{k}\cdot\vec{x}} + a_{\vec{k}}^\dagger \pi_{\vec{k}}^\star(\tau) e^{i\vec{k}\cdot\vec{x}}\right]. \qquad (2.2.17)$$

These are the small-wavelength parts of ϕ and π. The window function W turns off ($W \simeq 0$) for big wavelengths ($k \ll k_\sigma$) and turns on ($W \simeq 1$) for small wavelengths ($k \gg k_\sigma$). On the other hand, $\bar{\phi}$ and $\bar{\pi}$ are the long-wavelength (or coarse-grained) parts

of ϕ and π_ϕ. The operators $a_{\vec{k}}$ and $a_{\vec{k}}^\dagger$ are the usual annihilation and creation operators, satisfying the commutation relations $[a_{\vec{k}}, a_{\vec{k}'}^\dagger] = \delta^{(3)}(\vec{k} - \vec{k}')$ and $[a_{\vec{k}}, a_{\vec{k}'}] = [a_{\vec{k}}^\dagger, a_{\vec{k}'}^\dagger] = 0$. From now on, we shall only specify the norm k of the wave-number $\vec{k}$ because we will only be interested in isotropic initial states.

In Fourier space, equations (2.2.13) and (2.2.14) read

$$\dot{\phi}_k = \frac{N}{a^3}\pi_k, \tag{2.2.18}$$

$$\dot{\pi}_k = -Na^3 V_{,\phi\phi}\phi_k - k^2 Na\phi_k. \tag{2.2.19}$$

These expressions make up the full field and momentum operators in physical space given by $\Phi_{\vec{k}} = \phi_k(\tau)e^{-i\vec{k}\cdot\vec{x}}$ and $\Pi_{\vec{k}} = \pi_k(\tau)e^{-i\vec{k}\cdot\vec{x}}$. They are normalized through the Klein-Gordon inner product like

$$i\int_{\Sigma_\tau} \mathrm{d}^3 x (\Phi_{\vec{k}}\Pi_{\vec{k}'}^\star - \Pi_{\vec{k}}\Phi_{\vec{k}'}^\star) = \delta^{(3)}(\vec{k} - \vec{k}'), \tag{2.2.20}$$

where Σ_τ is a space-like hyper-surface of fixed time τ.

It is possible to obtain the Langevin equations for the long-wavelength parts $\bar{\phi}$ and $\bar{\pi}$ by plugging the decompositions $\phi = \bar{\phi} + \phi_Q$ and $\pi_\phi = \bar{\pi} + \pi_Q$ into (2.2.13) and (2.2.14) and linearising the result, i.e. keeping terms up to order 1 in quantum fluctuation. Doing this yields

$$\dot{\bar{\phi}} + \dot{\phi}_Q = \frac{N}{a^3}\left(\bar{\pi} + \pi_Q\right), \tag{2.2.21}$$

$$\dot{\bar{\pi}} + \dot{\pi}_Q = Na\Delta\phi_Q - Na^3\left[V_{,\phi} + V_{,\phi\phi}\phi_Q\right]. \tag{2.2.22}$$

In order to obtain this expression, the potential $V_{,\phi}(\phi)$ has been expanded about the coarse-grained value $\bar{\phi}$, so that $V_{,\phi}(\phi) = V_{,\phi}(\bar{\phi} + \phi_Q) \simeq V_{,\phi}(\bar{\phi}) + V_{,\phi\phi}(\bar{\phi})\phi_Q$ at leading order in ϕ_Q. Additionally, $\Delta\bar{\phi}$ has vanished since $\bar{\phi}$ is defined as a background value, meaning we do not expect a dependence on the point in space $\vec{x}$.

At this point we can plug in the definitions (2.2.16) and (2.2.17) of the quantum parts to obtain the Hamilton equations for the coarse-grained fields, which read

$$\dot{\bar{\phi}} = \frac{N}{a^3}\bar{\pi} + \xi_\phi(\tau), \tag{2.2.23}$$

$$\dot{\bar{\pi}} = -Na^3 V_{,\phi} + \xi_\pi(\tau), \tag{2.2.24}$$

where short-wavelength modes appear only through the quantum noises ξ_ϕ and ξ_π given by

$$\xi_\phi = -\int_{\mathbb{R}^3} \frac{\mathrm{d}^3 k}{(2\pi)^{3/2}}\dot{W}\left(\frac{k}{k_\sigma}\right)\left[a_{\vec{k}}\phi_{\vec{k}}(\tau)e^{-i\vec{k}\cdot\vec{x}} + a_{\vec{k}}^\dagger\phi_{\vec{k}}^\star(\tau)e^{i\vec{k}\cdot\vec{x}}\right], \tag{2.2.25}$$

$$\xi_\pi = -\int_{\mathbb{R}^3} \frac{\mathrm{d}^3 k}{(2\pi)^{3/2}}\dot{W}\left(\frac{k}{k_\sigma}\right)\left[a_{\vec{k}}\pi_{\vec{k}}(\tau)e^{-i\vec{k}\cdot\vec{x}} + a_{\vec{k}}^\dagger\pi_{\vec{k}}^\star(\tau)e^{i\vec{k}\cdot\vec{x}}\right]. \tag{2.2.26}$$

Notice that the quantum noises are proportional to the time derivative of the window function. This means that quantum effects are stronger in proximity of the quantum-to-classical transition.

2.2.3 Power spectrum

We shall work at linear order in perturbation theory and place both ϕ_k and π_k in their vacuum state. With these assumptions, the noises obey Gaussian statistics with vanishing mean. Their properties are fully specified by their two-points correlation matrix

$$\Xi(\tau_1, \vec{x}_1; \tau_2, \vec{x}_2) = \begin{pmatrix} \langle 0|\xi_\phi(\tau_1, \vec{x}_1)\xi_\phi(\tau_2, \vec{x}_2)|0\rangle & \langle 0|\xi_\phi(\tau_1, \vec{x}_1)\xi_\pi(\tau_2, \vec{x}_2)|0\rangle \\ \langle 0|\xi_\pi(\tau_1, \vec{x}_1)\xi_\phi(\tau_2, \vec{x}_2)|0\rangle & \langle 0|\xi_\pi(\tau_1, \vec{x}_1)\xi_\pi(\tau_2, \vec{x}_2)|0\rangle \end{pmatrix}. \qquad (2.2.27)$$

Inserting (2.2.25) and (2.2.26) into this expression leads to the matrix element

$$\Xi_{f_1 g_2} = \int_{\mathbb{R}^3} \frac{\mathrm{d}^3 k}{(2\pi)^{3/2}} \dot{W}\left(\frac{k}{k_\sigma(\tau_1)}\right) \dot{W}\left(\frac{k}{k_\sigma(\tau_2)}\right) f_k(\tau_1) g_k^\star(\tau_2) e^{i\vec{k}\cdot(\vec{x}_2 - \vec{x}_1)}, \qquad (2.2.28)$$

where we have introduced the notation $\Xi_{f_1 g_2} = \langle 0|\xi_f(\tau_1, \vec{x}_1)\xi_g(\tau_2, \vec{x}_2)|0\rangle$, with f and g being either ϕ or π.

Since we are only interested in isotropic states, we can turn to 3-dimensional polar coordinates and integrate over the angular variables, obtaining

$$\Xi_{f_1 g_2} = \int_{\mathbb{R}^+} \frac{k^2 \mathrm{d}k}{2\pi^2} \dot{W}\left(\frac{k}{k_\sigma(\tau_1)}\right) \dot{W}\left(\frac{k}{k_\sigma(\tau_2)}\right) f_k(\tau_1) g_k^\star(\tau_2) \frac{\sin(k|\vec{x}_2 - \vec{x}_1|)}{k|\vec{x}_2 - \vec{x}_1|}. \qquad (2.2.29)$$

At this point one needs to specify the window function W. The simplest and most natural choice is the Heaviside theta function $\theta(k/k_\sigma - 1)$. Its derivative is a Dirac delta distribution, so that $\dot{W}[k/k_\sigma(\tau_1)]\dot{W}[k/k_\sigma(\tau_2)] = \delta[k - k_\sigma(\tau_1)]\delta[k - k_\sigma(\tau_2)] = \delta(\tau_2 - \tau_1)$. Therefore we can solve the integral in (2.2.29) to obtain

$$\Xi_{f_1 g_2} = \frac{1}{6\pi^2} \left.\frac{\mathrm{d}k_\sigma^3(\tau)}{\mathrm{d}\tau}\right|_{\tau=\tau_1} f_k g_k^\star\Big|_{k=k_\sigma(\tau_1)} \frac{\sin[k_\sigma(\tau_1)|\vec{x}_2 - \vec{x}_1|]}{k_\sigma(\tau_1)|\vec{x}_2 - \vec{x}_1|} \delta(\tau_2 - \tau_1). \qquad (2.2.30)$$

We will only consider the autocorrelation of the noises, which is given by the approximation $\vec{x}_2 \simeq \vec{x}_1$, which means that $\sin[k_\sigma(\tau_1)|\vec{x}_2 - \vec{x}_1|]/[k_\sigma(\tau_1)|\vec{x}_2 - \vec{x}_1|] \simeq 1$. It is useful to write elements in the correlation matrix as $\Xi_{f_1 g_2}(\tau_1) = \Xi_{fg}(\tau_1)\delta(\tau_2 - \tau_1)$. On top of this, the power spectrum can be expressed in terms of the quantum fluctuations (recall f and g are ξ_ϕ and ξ_π) as

$$\mathcal{P}_{fg}(\tau, k) = \frac{k^3}{2\pi^2} f_k(\tau) g_k^\star(\tau). \qquad (2.2.31)$$

With this definition, the correlator matrix becomes

$$\Xi_{fg}(\tau) = \frac{d \ln[k_\sigma(\tau)]}{d\tau} \mathcal{P}_{fg}[\tau, k_\sigma(\tau)]. \tag{2.2.32}$$

Often times, it is convenient to work with the symmetric part of Ξ, which will be defined as the diffusion matrix D, given by

$$D = \frac{\Xi_{\phi\phi} + \Xi_{\pi\pi}}{2} I + \frac{\Xi_{\phi\pi} + \Xi_{\pi\phi}}{2} J_x + \frac{\Xi_{\phi\phi} - \Xi_{\pi\pi}}{2} J_z, \tag{2.2.33}$$

where I is the 2-dimensional identity matrix and $\{J_x, J_y, J_z\}$ are the 2-dimensional Pauli matrices.

2.2.4 Solution for a free scalar field

In this section we will assume that the inflaton is driven by a quadratic potential $V(\phi) = \Lambda^4 + m^2\phi^2/2$. This assumption may seem too strong and rule out more realistic potentials. However, regardless of the model, we can expand the potential about an arbitrary point and stop at second order (first order can often be neglected due to shift symmetry). Since this potential only features a constant term and a mass term, the field ϕ is a free scalar field. Let us assume the noises ξ_ϕ and ξ_π do not depend on the phase-space variables $\bar{\phi}$ and $\bar{\pi}$ of the coarse-grained field. Then equations (2.2.23) and (2.2.24) form a linear differential system, which can be analytically solved.

Since the system formed by (2.2.23) and (2.2.24) is linear, it is useful to introduce the vector notation

$$\Phi = \begin{pmatrix} \bar{\phi} \\ \bar{\pi} \end{pmatrix}, \qquad \xi = \begin{pmatrix} \xi_\phi \\ \xi_\pi \end{pmatrix}. \tag{2.2.34}$$

This means that the system formed by (2.2.23) and (2.2.24) can be compactly written as

$$\dot{\Phi} = A(\tau)\Phi + \xi(\tau), \tag{2.2.35}$$

where

$$A(\tau) = \begin{pmatrix} 0 & N/a^3 \\ -m^2 N a^3 & 0 \end{pmatrix}. \tag{2.2.36}$$

A standard result of the stochastic formalism is the Fokker-Planck equation. It allows us to find a probability density function (PDF) $P(\tau, \Phi)$ in phase space starting from the Langevin equations (2.2.35). It is a differential equation in $P(\tau, \Phi)$ and reads

$$\frac{\partial P(\tau, \Phi)}{\partial \tau} = -\sum_{i,j=1}^{2} \frac{\partial}{\partial \Phi_i} [A_{ij}\Phi_j P(\tau, \Phi)] + \frac{1}{2} \sum_{i,j=1}^{2} \frac{\partial^2}{\partial \Phi_i \partial \Phi_j} [\Xi_{ij}(\tau) P(\tau, \Phi)]. \tag{2.2.37}$$

In this expression the first term is called the drift term and it is responsible for the deterministic part of dynamics. On the other hand, the second term, called the diffusive term, traces the stochastic part.

Expression (2.2.37) can be further simplified because of the simplicity of our initial assumptions, reaching the final result

$$\frac{\partial P(\tau, \Phi)}{\partial \tau} = - \sum_{i,j=1}^{2} \frac{\partial}{\partial \Phi_i} \left[A_{ij} \Phi_j P(\tau, \Phi) \right] + \frac{1}{2} \sum_{i,j=1}^{2} D_{ij}(\tau) \frac{\partial^2 P(\tau, \Phi)}{\partial \Phi_i \partial \Phi_j}, \qquad (2.2.38)$$

where $D(\tau)$ is the symmetric part of Ξ as defined in (2.2.33). This equation tells us that in order to fully determine the stochastic properties of our system, all we need to evaluate is the matrix D.

Explicit solution in a de-Sitter background

Let us now find an explicit solution to the Hamiltonian system formed by (2.2.18) and (2.2.19). We will choose to work with number of e-folding, so that $N = 1/H$. The Hamiltonian system mentioned above leads to the equation of motion

$$\phi_{k,N_e N_e} + (3 - \epsilon)\phi_{k,N_e} + \left[\left(\frac{k}{aH} \right)^2 + \frac{V_{,\phi\phi}}{H^2} \right] \phi_k = 0, \qquad (2.2.39)$$

where $, N_e$ indicates derivation with respect to number of e-foldings.

Let us work out the case of a massless scalar field evolving in a perfect de-Sitter background $V(\phi) = \Lambda^4$. This means $V_{,\phi\phi} = 0$ and $\epsilon = 0$, since the potential is simply a cosmological constant and the Hubble constant is strictly constant. The solution reads

$$\phi_x = x^{3/2} \left[\alpha H_{3/2}^{(1)}(x) + \beta H_{3/2}^{(2)}(x) \right], \qquad (2.2.40)$$

where we have set $x = k/(aH)$ for convenience; $H_n^{(1,2)}$ are Hankel functions of the first and second kind respectively; α and β are integration constants. Their value can be found by imposing suitable initial conditions. We will assume Bunch-Davies initial conditions, which means that

$$\lim_{x \to \infty} \phi_x = \frac{e^{-ix}}{a\sqrt{2xaH}}. \qquad (2.2.41)$$

In order to compare this limit to our solution (2.2.40), we need to evaluate (2.2.40) when $x \gg 1$. A quick calculation shows that

$$\lim_{x \to \infty} \phi_x = -\sqrt{\frac{2}{\pi}} \alpha x e^{ix} - \sqrt{\frac{2}{\pi}} \beta x e^{-ix}. \qquad (2.2.42)$$

In order for this expansion to agree with the Bunch-Davies condition (2.2.41), the negative frequency coefficient must vanish $\alpha = 0$, and the positive frequency coefficient must satisfy

$$\beta = -\frac{H\sqrt{\pi}}{2k^{3/2}}. \tag{2.2.43}$$

This leaves us with the fully determined solution

$$\phi_k = -\frac{H\sqrt{\pi}}{2(aH)^{3/2}}H_{3/2}^{(2)}\left(\frac{k}{aH}\right)$$
$$= \frac{1}{a\sqrt{2k}}\left(1 - \frac{iaH}{k}\right)e^{-ik/(aH)}, \tag{2.2.44}$$

where the last step was obtained by using Hankel function identities. Using (2.2.18) one can find the conjugated momentum

$$\pi_k = Ha^3\dot{\phi}_k$$
$$= ia\sqrt{\frac{k}{2}}e^{-ik/(aH)}. \tag{2.2.45}$$

It is now convenient to introduce the cut-off wavelength $k_\sigma = \sigma aH$ by substituting $k \mapsto k_\sigma$. Recalling definition (2.2.33), the diffusion matrix in de-Sitter space with wavelength cut-off is given by

$$D = \begin{pmatrix} \frac{H^2(1+\sigma^2)}{4\pi^2} & -\frac{a^3H^3\sigma^2}{4\pi^2} \\ -\frac{a^3H^3\sigma^2}{4\pi^2} & \frac{a^6H^4\sigma^4}{4\pi^2} \end{pmatrix}. \tag{2.2.46}$$

Notice that, in the physical limit $\sigma \ll 1$, the scalar field direction in the diffusion matrix correctly reproduces the familiar result $D_{\phi\phi} \simeq D_{\phi\phi}^{\mathrm{SR}} = H^2/4\pi^2$.

Explicit solution in a slow-roll background

Let us now generalise the results of the previous calculation to a slow-roll inflationary background. The potential is no longer constant, therefore $V_{,\phi\phi}$ is now a function of ϕ. However, as previously pointed out, an expansion of the potential $V(\phi)$ about for example the coarse-grained field $\bar{\phi}$ will make the coefficient $V_{,\phi\phi}$ a simple constant. Let us define the index

$$\nu = \frac{3}{2}\sqrt{1 - \frac{4V_{,\phi\phi}}{9H^2}}. \tag{2.2.47}$$

Equation (2.2.39) is solved by

$$\phi_x = x^{3/2}\left[\alpha H_\nu^{(1)}(x) + \beta H_\nu^{(2)}(x)\right], \tag{2.2.48}$$

which generalises (2.2.40). Again, α and β are found by imposing initial Bunch-Davies conditions and comparing the condition to the expansion for the solution (2.2.48) about $x \gg 1$. While α is found to vanish even in this more general case, this time β is given by

$$\beta = i \frac{H \sqrt{\pi}}{2k^{3/2}} e^{-i \frac{\pi}{4}(2\nu+3)}. \tag{2.2.49}$$

Bear in mind the phase factor is completely irrelevant, because all physical quantities depend on $|\phi|^2$. Nevertheless, it will be kept throughout the calculations for completeness' sake. The solution then is given by

$$\phi_k = i \frac{H \sqrt{\pi}}{2(aH)^{3/2}} e^{-i \frac{\pi}{4}(2\nu+3)} H_\nu^{(2)} \left(\frac{k}{aH} \right), \tag{2.2.50}$$

whose conjugated momentum is

$$\pi_k = \frac{a \sqrt{aH} \sqrt{\pi}}{4} e^{-i \frac{\pi}{4}(2\nu-3)} \left[\frac{2k}{aH} H_{\nu-1}^{(2)} \left(\frac{k}{aH} \right) + (3 - 2\nu) H_\nu^{(2)} \left(\frac{k}{aH} \right) \right]. \tag{2.2.51}$$

As usual, we will utilise the cut-off $k_\sigma \mapsto \sigma aH$. This time the matrix elements of the symmetric part D of the correlator matrix involve more complicated terms. They are given by [1]

$$
D_{\phi\phi} = \frac{H^2 \Gamma(\nu)^2}{\pi^3} \left(\frac{\sigma}{2} \right)^{3-2\nu} \left\{ 1 + \frac{2}{\nu - 1} \left(\frac{\sigma}{2} \right)^2 \right.
$$
$$
\left. - \frac{2\pi \nu^2 \cot(\pi\nu)}{\Gamma(\nu)\Gamma(\nu+1)} \left(\frac{\sigma}{2} \right)^{2\nu} + \frac{2\nu - 3}{(\nu-2)(\nu-1)^2} \left(\frac{\sigma}{2} \right)^4 + \mathcal{O}(\sigma^5) \right\}, \tag{2.2.52}
$$

$$
D_{\pi\pi} = \frac{a^6 H^4 \Gamma(\nu)^2}{4\pi^3} \left(\frac{\sigma}{2} \right)^{3-2\nu} \left\{ (2\nu - 3)^2 + \frac{2(2\nu-3)(2\nu-7)}{\nu - 1} \left(\frac{\sigma}{2} \right)^2 \right.
$$
$$
+ \frac{2\pi \cot(\pi\nu)(2\nu-3)(2\nu+3)}{\Gamma(\nu)\Gamma(\nu+1)} \left(\frac{\sigma}{2} \right)^{2\nu}
$$
$$
\left. + \frac{8\nu^3 - 68\nu^2 + 166\nu - 131}{(\nu-2)(\nu-1)^2} \left(\frac{\sigma}{2} \right)^4 + \mathcal{O}(\sigma^5) \right\}, \tag{2.2.53}
$$

$$
D_{\phi\pi} = D_{\pi\phi} = \frac{a^3 H^3 \Gamma(\nu)^2}{\pi^3} \left(\frac{\sigma}{2} \right)^{3-2\nu} \left\{ 2\nu - 3 + \frac{2(2\nu-5)}{\nu-1} \left(\frac{\sigma}{2} \right)^2 \right.
$$
$$
\left. + \frac{6\pi \cot(\pi\nu)}{\Gamma(\nu)\Gamma(\nu+1)} \left(\frac{\sigma}{2} \right)^{2\nu} + \frac{(2\nu-3)(2\nu-7)}{(\nu-2)(\nu-1)^2} \left(\frac{\sigma}{2} \right)^4 + \mathcal{O}(\sigma^5) \right\}. \tag{2.2.54}
$$

This expansion was obtained and ordered assuming $1 < \nu < 2$. One can easily compare these expressions with (2.2.46) and see that (2.2.46) is precisely reproduced when

---

[1]Some of the coefficients multiplying $(\sigma/2)^{2\nu}$ terms are in disagreement with what was found by [10]. However, they are sub-leading terms in slow-roll and they are not expected to affect dynamics greatly.

we plug $\nu = 3/2$ into (2.2.52), (2.2.53) and (2.2.54). In order for this correspondence to be evident, we have shown terms up to σ^4 even though this is not necessary in practice given that only leading terms in σ are required to be kept in the stochastic classical approximation.

Additionally, the limit $\sigma \to 0$ again correctly reproduces the de Sitter approximation $D_{\phi\phi} \simeq D_{\phi\phi}^{\text{SR}} = H^2/4\pi^2$. While the other entries in the matrix vanish in the massless case, this is no longer true in the general case. Indeed, $D_{\pi\pi}$ and $D_{\phi\pi}$ feature sub-leading terms in σ.

2.3 Overview of the literature

In the present section we summarise three articles that make use of the stochastic formalism introduced in section 2.2 and that have conflicting assumptions and conclusions regarding the role of stochastic effects in ultra slow-roll and primordial black hole formation.

2.3.1 De Sitter noise

In this section we will report the steps taken by [11] to justify their claim that quantum diffusion does play a significant role in determining the abundance of PBHs today.

Let us expand the scalar potential around the value ϕ_0 at which the scalar field enters USR, such that

$$V(\phi) \simeq V_0\big(1 + \sqrt{2\epsilon_V}(\phi - \phi_0)\big) + \cdots, \tag{2.3.1}$$

where $\sqrt{2\epsilon_V} = V_{,\phi}/V_0$. This expansion is valid in the range $\phi_\star < \phi < \phi_0$, where $\phi_\star$ is the value of the inflaton field at the end of the USR phase. We arbitrarily define $N_e = 0$ the beginning of the USR phase with initial conditions $\phi(0) = \phi_0$ and $\mathrm{d}\phi/\mathrm{d}N_e\big|_{N_e=0} = \Pi_0$. In this simple scenario, the equation of motion reads

$$\phi_{,N_e N_e} + 3\phi_{,N_e} + \frac{V_{,\phi}}{H^2} = 0, \tag{2.3.2}$$

approximating $3 - \epsilon \simeq 3$. Using $H^2 \simeq V/3$, the solution reads

$$\phi(N_e) = \phi_0 + \frac{1}{3}[\Pi_0 - \Pi(N_e)] - \sqrt{2\epsilon_V}N_e, \tag{2.3.3}$$

$$\Pi(N_e) = \Pi_0 e^{-3N_e} + \sqrt{2\epsilon_V}(e^{-3N_e} - 1), \tag{2.3.4}$$

where $\Pi(N) = \mathrm{d}\phi(N_e)/\mathrm{d}N_e$.

Equation (2.3.4) tells us that the inflaton's velocity exponentially decays after entering the USR phase. Indicating by $\Pi_\star$ the value of the velocity at the end of this phase,

the curvature perturbation is given by

$$\zeta_\star = -\frac{\phi_k}{\Pi}\bigg|_{N_e = N_e^\star},\tag{2.3.5}$$

where $\phi_k = H/\sqrt{2k^3}$. Even though the slow-roll condition is strongly violated, this still results in a flat power spectrum, since

$$\mathcal{P}_{\zeta_\star} = \frac{k^3}{2\pi^2}|\zeta_\star|^2 = \frac{H^2}{4\pi^2\Pi_\star^2}.\tag{2.3.6}$$

This is due to a particular dual symmetry enjoyed by the system in question.

So far we have discussed modes that cross the horizon towards the end of the USR phase. Let us now discuss what happens to those modes that leave the Hubble radius during the sudden transition from slow-roll to USR. It can be shown that, for those modes, the power spectrum looks like [11]

$$\mathcal{P}_{\zeta_k} = g(-k\tau_0)\mathcal{P}_{\zeta_\star},\tag{2.3.7}$$

$$\begin{aligned}g(x) = \frac{1}{2x^6}\Big[&9 + 18x^2 + 9x^4 + 2x^6 + 3\left(-3 + 7x^4\right)\cos(2x)\\ &- 6x\left(3 + 4x^2 - x^4\right)\sin(2x)\Big],\end{aligned}\tag{2.3.8}$$

where we have turned to cosmic time and τ_0 represents the moment when the USR phase begins. Since figure 2.1 shows a peak for $g(x)$ of about 2.5, we can say that

$$\mathcal{P}_{\zeta_{\text{peak}}} \simeq 2.5\mathcal{P}_{\zeta_\star} = 2.5\left(\frac{H_\star}{2\pi\Pi_\star}\right)^2.\tag{2.3.9}$$

An example: Starobinsky model

Let us now introduce a potential first described by Starobinsky [17]. It features two distinct slow-roll phases, linked by a very short phase in which $|\eta| \sim \mathcal{O}(1)$. In the following, we will use the parametrization used by [11]:

$$\begin{aligned}V(\phi) = V_0\Big[&1 + \frac{1}{2}\left(\sqrt{2\epsilon_+} - \sqrt{2\epsilon_-}\right)(\phi - \phi_c)\tanh\left(\frac{\phi - \phi_c}{\delta}\right)\\ &+ \frac{1}{2}\left(\sqrt{2\epsilon_+} + \sqrt{2\epsilon_-}\right)(\phi - \phi_c)\Big],\end{aligned}\tag{2.3.10}$$

where δ is proportional to the duration of the transition and $\epsilon_- \ll 1$, $\epsilon_+ \ll 1$ are the slow-roll parameters before and after the transition respectively. A detailed discussion on the form of this potential is delayed until section 3.1.
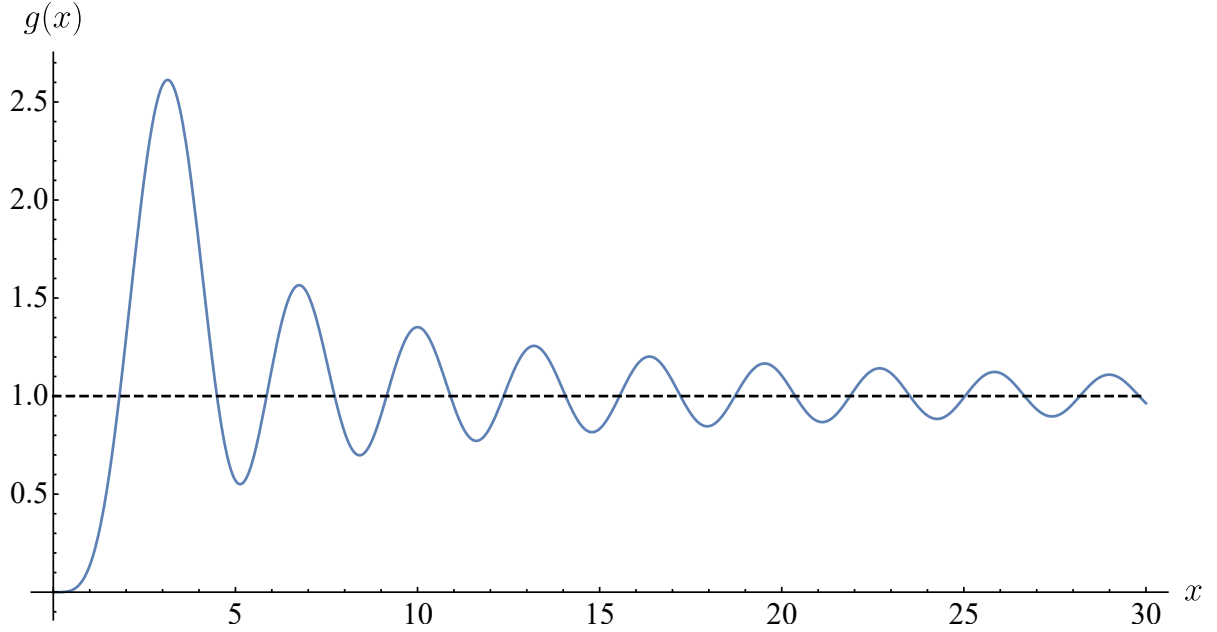
33

Figure 2.1: Function used to write $\mathcal{P}_{\zeta_k}$ for those modes that leave the Hubble radius during the sudden transition from slow-roll to USR in terms of $\mathcal{P}_{\zeta_\star}$.

Probability density functions

Recall that the power spectrum depends on the inverse of the inflaton velocity. When we take quantum diffusion into account, we need to consider that the inflaton velocity cannot deviate too much from its classical value, since it would not give rise to a correct power spectrum enhancement, failing to reproduce the desired PBH abundance. This means that the spread in inflaton velocity cannot be too large and needs to be carefully scrutinised. For this reason, let us turn our attention to solving the stochastic equation of motion for the scalar field ϕ given by

$$\phi_{,N_e N_e} + 3\phi_{,N_e} + \frac{V_{,\phi}}{H^2} = \xi, \tag{2.3.11}$$

which is (2.3.2) with its inhomogeneous part given by the random Gaussian noise $\xi(\tau)$. This problem can be reformulated as an Ornstein-Uhlenbeck process where

$$\phi_{,N_e} = \Pi,$$
$$\Pi_{,N_e} + 3\Pi + \frac{V_{,\phi}}{H^2} = \xi,$$
$$\langle \xi(N_e)\xi(N'_e) \rangle = D\delta(N_e - N'_e), \tag{2.3.12}$$
$$D = \frac{9H^2}{4\pi^2}.$$

Note that the two-point function of the random Gaussian noise is nothing but (2.2.27) where we take the exact de Sitter approximation for the noise correlator matrix. The Kramers-Moyal (KM) equation that generalises the Focker-Planck equation (2.2.37) for the corresponding probability density function $P = P(\phi, \Pi, N_e)$ is

$$\frac{\partial P}{\partial N_e} = -\frac{\partial}{\partial \phi}(\Pi P) + \frac{\partial}{\partial \Pi}\left(\mathcal{V}_{,\Pi}P + \frac{V_{,\phi}}{H^2}P\right) + \frac{D}{2}\frac{\partial^2}{\partial \Pi^2}P, \qquad (2.3.13)$$

where $\mathcal{V} = 3\Pi^2/2$. The initial condition for the probability is

$$P(\phi, \Pi, 0) = \delta(\phi - \phi_c)\delta(\Pi - \Pi_c). \qquad (2.3.14)$$

This is because it has been assumed that quantum diffusion has a negligible effect before the transition phase. At number of e-foldings $N_e \gtrsim 1$, the solution to (2.3.13) is approximately given by

$$P(\phi, \Pi, N_e) \simeq \frac{1}{\Pi}\left(\frac{27}{2D^2 N_e}\right)^{1/2}$$
$$\exp\left[-\frac{9}{2DN_e}(\Delta\phi)^2\right]\exp\left[\frac{3}{DN_e}\Delta\phi\Delta\Pi\right]\exp\left[-\frac{3}{D}(\Delta\Pi)^2\right]. \qquad (2.3.15)$$

We can now integrate over Π to obtain

$$P_\phi(N_e) = \frac{3}{\sqrt{2\pi D N_e}}\exp\left[-\frac{9}{2DN_e}(\phi - \phi(N_e))^2\right]. \qquad (2.3.16)$$

The variance in the scalar field therefore is

$$\langle\Delta\phi^2\rangle = \int \mathrm{d}\phi(\phi - \phi(N_e))^2 P_\phi(N_e) = \frac{D}{9}N_e. \qquad (2.3.17)$$

On the other hand, integrating over ϕ yields

$$P_\Pi(N_e) = \sqrt{\frac{3}{\pi D}}\exp\left[-\frac{3}{D}(\Pi - \Pi(N_e))^2\right], \qquad (2.3.18)$$

with variance

$$\langle\Delta\Pi^2\rangle = \int \mathrm{d}\Pi(\Pi - \Pi(N_e))^2 P_\Pi(N_e) = \frac{D}{6}. \qquad (2.3.19)$$

This means that when the inflaton field decays, its velocity quickly reaches an asymptotic value.

Gauging the effects on the PBH abundance

At this point, the authors of [11] run a numerical simulation that involves generating a large number of Universes with different values for the inflaton field velocity in USR. It is considered a quantum field with Gaussian distribution centred around its classical value $\Pi_\star$ with variance $\langle \Delta \Pi^2 \rangle$. They test a linear and a Starobinsky potential and confirm that what they find is in agreement with the theoretical result (2.3.19). More realistic potentials, such as the one described in [14], are in agreement with a more precise version (see [11] for more details) of (2.3.19) that involves the slow-roll parameter η.

The spread in inflaton field velocity is of the utmost importance when trying to calculate PBH abundance. If the variance $\langle \Delta \Pi^2 \rangle^{1/2}$ is smaller than the size $\delta \Pi_\star$ of the region over which the curvature perturbation is of order $\mathcal{P}_{\zeta_{\mathrm{peak}}}^{1/2}$, the wave packet is tightly compacted about this region and most trajectories will display the same power spectrum. This means one needs to impose the condition

$$\frac{\langle \Delta \Pi^2 \rangle^{1/2}}{H} \ll \frac{\delta \Pi_\star}{H} \tag{2.3.20}$$

if we want all curvature perturbations ζ_k at a scale k to generate a power spectrum $\mathcal{P}_{\zeta_k}$ such that $\mathcal{P}_{\zeta_k} \sim \mathcal{P}_{\zeta_{\mathrm{peak}}}$.

Let us test condition (2.3.20) for a linear potential. Since $\mathcal{P}_{\zeta_{\mathrm{peak}}} \sim 2.5 \mathcal{P}_{\zeta_\star}$, definition (2.3.6) tells us that

$$\delta \Pi_\star \simeq 1.6 \frac{H_\star}{2\pi \mathcal{P}_{\zeta_{\mathrm{peak}}}^{1/2}}. \tag{2.3.21}$$

Therefore, criterion (2.3.20) means that

$$\mathcal{P}_{\zeta_{\mathrm{peak}}}^{1/2} \ll 1.6 \frac{H_\star}{2\pi \langle \Delta \Pi^2 \rangle^{1/2}}, \tag{2.3.22}$$

Now, making use of (2.3.19) leads to

$$\mathcal{P}_{\zeta_{\mathrm{peak}}}^{1/2} \ll 1.6 \sqrt{\frac{2}{3}} \simeq 1.3. \tag{2.3.23}$$

This condition is used to gauge the role of quantum diffusion on the enhancement of the power spectrum. The peak in the power spectrum required to generate the correct abundance of PBHs is $\sim \mathcal{O}(10^{-2})$. This means that (2.3.23) is satisfied. However, as we will show shortly, this does not seem enough to imply that quantum effects are expected to be negligible in the determination of the PBH abundance.

In the more realistic case, the same analysis can be carried out. This time, it was estimated numerically by [11] that $\mathcal{P}_{\zeta_{\mathrm{peak}}}^{1/2} \sim 7 H_\star / (2\pi \Pi_\star)$. They find

$$\frac{\delta \Pi_\star}{H} \simeq 1.4, \tag{2.3.24}$$

while

$$\frac{\langle \Delta \Pi^2 \rangle^{1/2}}{H} \simeq 0.4. \tag{2.3.25}$$

Criterion (2.3.20) is still comfortably satisfied even in this case.

A stronger criterion than (2.3.20) directly involving the PBH abundance $\beta_{\mathrm{f}}(M)$ introduced in section 2.1 can be derived. Recall that $\beta_{\mathrm{f}}(M)$ is the fraction of total energy in PBHs and it is given by

$$\beta_{\mathrm{f}}(M) \simeq \frac{\sigma_M}{\sqrt{2\pi}\zeta_{\mathrm{c}}} e^{-\frac{\zeta_{\mathrm{c}}^2}{2\sigma_M^2}}. \tag{2.3.26}$$

Quantum diffusion needs to be precisely fine-tuned, because any slight variation from the correct spread in inflaton velocities will result in a huge change in PBH abundance. We will then consider the spread in the PBH energy fraction itself.

Let us promote $\beta_{\mathrm{f}}(M)$ to a quantum variable and consider the case of a linear potential. Its average value is given by

$$\langle \beta_{\mathrm{f}}(M) \rangle = \int \mathrm{d}\Pi P_\Pi(N_e) \beta_{\mathrm{f}}(M)$$
$$= \frac{\sigma_M}{\sqrt{2\pi}(1+\theta)^{3/2}\zeta_{\mathrm{c}}} e^{-\frac{\zeta_{\mathrm{c}}^2}{2(1+\theta)\sigma_M^2}}, \tag{2.3.27}$$

where $\theta = 4\pi^2 \zeta_{\mathrm{c}}^2 \langle \Delta \Pi^2 \rangle / H^2$. Recall that the probability distribution $P_\Pi(N_e)$ is defined in (2.3.18). Let us introduce the quantity Δ_{qd} such that

$$\frac{\langle \beta_{\mathrm{f}} \rangle}{\beta_{\mathrm{f}}} = e^{\Delta_{\mathrm{qd}}}. \tag{2.3.28}$$

This quantity tells us how far that abundance of PBH calculated in the classical framework differs from the quantum one. Using equation (2.3.27) takes us to

$$\Delta_{\mathrm{qd}} \simeq -\frac{\zeta_{\mathrm{c}}^2}{2\sigma_M^2} \left(\frac{\theta}{\theta - 1} \right). \tag{2.3.29}$$

It is reasonable to assume that the classical calculation does not stray too far from the full quantum one when $\Delta_{\mathrm{qd}} \lesssim 1$. This means that

$$\frac{\langle \Delta \Pi^2 \rangle^{1/2}}{H} \lesssim \frac{\sigma_M}{\sqrt{2\pi}\zeta_{\mathrm{c}}^2} \simeq 10^{-2} \left(\frac{\sigma_M}{0.1} \right) \left(\frac{1.3}{\zeta_{\mathrm{c}}} \right)^2. \tag{2.3.30}$$

This condition is badly violated by a spread $\sqrt{D/6}/H \simeq 0.2$. One can alternatively fix the required PBH abundance $\beta_{\mathrm{f}} \simeq 10^{-16}$ and find a lower bound on the variance

$$\sigma_M \gtrsim 2 \left(\frac{\zeta_{\mathrm{c}}}{1.3} \right)^2. \tag{2.3.31}$$

This condition, in contrast to (2.3.23), is not easy to satisfy, indicating the difficulty of ignoring the impact of quantum diffusion on power spectrum enhancement.

37

2.3.2 Enhanced noise

In the following sections we will take on the point of view of [12]. We will first review their formalism, then report on their findings. Finally, we will comment on a few of their results.

The authors of [12] work with a toy potential whose general shape closely resembles that of [14]. Their analysis begins with solving the evolution equation for quantum fluctuations ζ_k, given by the Mukhanov-Sasaki equation. This will allow us to calculate the primordial power spectrum. Let us briefly remind the definition

$$\zeta = \frac{u}{z} = \frac{a\delta\phi}{z}, \qquad (2.3.32)$$

where u is the Mukhanov-Sasaki variable and $z = a\dot{\phi}$. In Fourier space, the evolution equation is

$$\zeta_{k,N_eN_e} + (3 - \epsilon + \eta)\zeta_{k,N_e} + \left(\frac{k}{aH}\right)^2 \zeta_k = 0, \qquad (2.3.33)$$

where $\zeta_k = u_k/z$. This equation is easily obtained from the Mukhanov-Sasaki equation $u_k''(\eta) + (k^2 - z''/z)u_k = 0$ expressed in number of e-foldings rather than conformal time. Notice this equation has two regimes delimited by $k/(aH)$. At sub-horizon scales $k/(aH) \gg 1$, the friction term becomes negligible and the field behaves as a free field in Minkowski space. At super-horizon scales $k/(aH) \ll 1$ the friction term dominates over all other terms, and the solution can be found by considering

$$\left.\frac{\mathrm{d}\zeta_k}{\mathrm{d}N_e}\right|_{k/(aH)\ll 1} = \tilde{C}_2 \exp\left[-\int \mathrm{d}N_e(3 - \epsilon + \eta)\right] = C_2 \exp[-3N_e + \ln H - \ln\epsilon], \quad (2.3.34)$$

which implies

$$\zeta_k\big|_{k/(aH)\ll 1} = C_1 + C_2 \int \mathrm{d}N_e e^{-3N_e + \ln H - \ln\epsilon}. \qquad (2.3.35)$$

This tells us that there is one constant mode and one evolving mode. The second one is either growing or decaying depending on the sign of the exponent $-3N_e + \ln H - \ln\epsilon$.

These modes allow us to calculate the power spectrum

$$\mathcal{P}_\zeta^{\mathrm{MS}} = \frac{k^3}{2\pi^2}|\zeta_k|^2\bigg|_{k/(aH)\ll 1}. \qquad (2.3.36)$$

Now, the time-dependent mode in (2.3.35) is usually negligible since for small ϵ and η it corresponds to a decaying solution. This means that the curvature perturbation ζ_k can be considered constant after horizon crossing. Therefore, the power spectrum can be safely evaluated at horizon crossing $k = aH$. This brings us to

$$\mathcal{P}_\zeta^{\mathrm{SR}} \simeq \frac{1}{8\pi^2 M_{\mathrm{Pl}}^2} \frac{V(\phi)}{\epsilon(3 - \epsilon)}, \qquad (2.3.37)$$
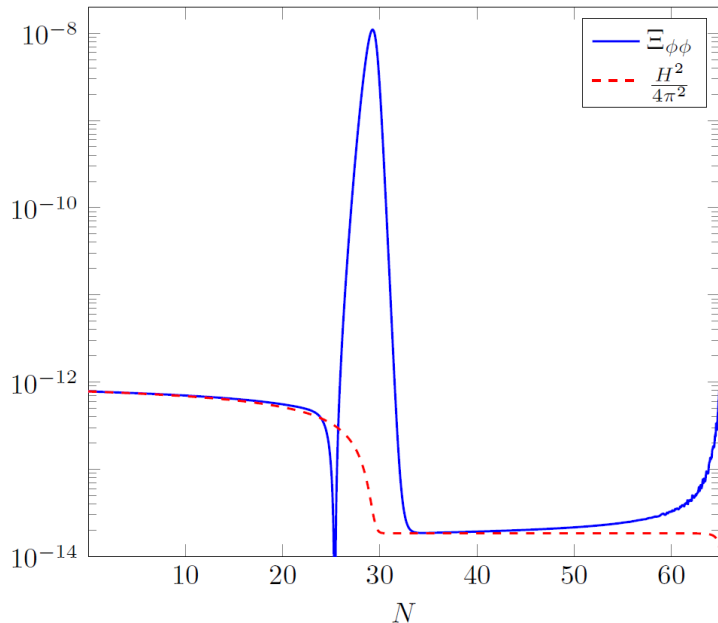
38

Figure 2.2: Enhancement of the stochastic correlator noise $\Xi_{\phi\phi}$ for modes that leave the horizon during USR. The slow-roll approximation is still valid for those that leave well before or well after the USR phase. This picture was taken from [12].

where the approximation is valid as long as slow-roll holds. This result gives us an intuition as to what needs to be done in order to achieve power spectrum enhancement: slow down the inflaton so that ϵ takes small values.

However, beyond slow-roll, the friction term might flip sign. This happens when $\eta < -3 + \epsilon$, and the mode which was decaying will now grow, inducing a growth in the curvature perturbation, as seen in figure 2.2. This, in turn, causes the power spectrum to rapidly grow. This is the main mechanism leading to power spectrum enhancement in single field inflation models.

This behaviour is confirmed by our analysis in chapter 3 as well: modes that leave the horizon around the time when $|\eta| \sim \mathcal{O}(1)$ enjoy a rapid growth. Those that leave the horizon well after this transition though, are mostly unaffected and behave as if the transition never occurred.

At this point, the authors of [12] make use of the very same stochastic formalism already presented in section 2.2: they split the field and its momentum in their coarse-grained and quantum parts, then solve the Langevin equations. However they take a different approach when they calculate the power spectrum. A general correlation function is defined as

$$\langle \delta\phi^n \delta\pi^m \rangle (N_e) = \int \mathrm{d}\bar{\pi}_\phi \int \mathrm{d}\bar{\phi} (\bar{\phi} - \phi_{\mathrm{cl}}(N_e))^n (\bar{\pi}_\phi - \pi_{\mathrm{cl}}(N_e))^m P(N_e, \Phi), \qquad (2.3.38)$$

where the quantum solution to the Langevin equation was expanded about its classical trajectory such that

$$\delta\phi = \bar{\phi} - \phi_{\text{cl}}, \tag{2.3.39}$$

$$\delta\pi = \bar{\pi}_\phi - \pi_{\text{cl}}. \tag{2.3.40}$$

It can be checked that the probability density function $P(N_e, \Phi)$ satisfies the Focker-Planck equation

$$\frac{\partial P(N_e, \Phi)}{\partial N_e} = -\frac{\partial}{\partial \Phi_f}\left(D_f P(N_e, \Phi) - \frac{\Xi_{fg}}{2}\frac{\partial P(N_e, \Phi)}{\partial \Phi_g}\right), \tag{2.3.41}$$

which is equivalent to (2.2.38). Here, the indices f and g refer to $\bar{\phi}$ and $\bar{\pi}_\phi$, repeated indices indicate summation and D is the drift vector with components

$$D_\phi = \bar{\pi}_\phi,$$
$$D_\pi = -(3 - \epsilon)\left[\bar{\pi}_\phi + M_{\text{Pl}}^2(\ln V)_{,\phi}\right]. \tag{2.3.42}$$

Taking the N_e derivative of (2.3.38) and using the Focker-Planck equation (2.2.38) yields

$$\begin{aligned}
\frac{\mathrm{d}}{\mathrm{d}N_e}\langle\delta\phi^n\delta\pi^m\rangle &= n\left(\langle\delta\phi^{n-1}\delta\pi^m D_\phi\rangle - \langle\delta\phi^{n-1}\delta\pi^m\rangle D_\phi^{\text{cl}}\right) \\
&\quad + m\left(\langle\delta\phi^n\delta\pi^{m-1} D_\pi\rangle - \langle\delta\phi^n\delta\pi^{m-1}\rangle D_\pi^{\text{cl}}\right) \\
&\quad + \frac{1}{2}n(n-1)\Xi_{\phi\phi}\langle\delta\phi^{n-2}\delta\pi^m\rangle + \frac{1}{2}m(m-1)\Xi_{\pi\pi}\langle\delta\phi^n\delta\pi^{m-2}\rangle \\
&\quad + \frac{1}{2}nm(\Xi_{\phi\pi} + \Xi_{\pi\phi})\langle\delta\phi^{n-1}\delta\pi^{m-1}\rangle,
\end{aligned} \tag{2.3.43}$$

where D_ϕ^{cl} and D_π^{cl} are the drift terms (2.3.42) evaluated at classical trajectory. In theory, one has to solve the infinite differential system formed by (2.3.43) in order to find the full time evolution of each correlation function. In practice, one can truncate the system at a certain point and consider higher moments negligible.

The power spectrum is closely related to the 2-point correlation functions. At leading order, the evolution equations (2.3.43) for n and m up to 1 can be organised as follows

$$\frac{\mathrm{d}}{\mathrm{d}N_e}\begin{pmatrix}\langle\delta\phi^2\rangle \\ \langle\delta\phi\delta\pi\rangle \\ \langle\delta\pi^2\rangle\end{pmatrix} = \begin{pmatrix} 0 & -2 & 0 \\ g(\epsilon_n) & -f(\epsilon_n) & -1 \\ 0 & 2g(\epsilon_n) & -2f(\epsilon_n)\end{pmatrix}\begin{pmatrix}\langle\delta\phi^2\rangle \\ \langle\delta\phi\delta\pi\rangle \\ \langle\delta\pi^2\rangle\end{pmatrix} + \begin{pmatrix}\Xi_{\phi\phi} \\ \Xi_{\phi\pi}^{\text{symm}} \\ \Xi_{\pi\pi}\end{pmatrix}, \tag{2.3.44}$$

where $\Xi_{\phi\pi}^{\text{symm}} = (\Xi_{\phi\pi} + \Xi_{\pi\phi})/2$ and

$$f(\epsilon_n) = 3 - \epsilon_1\left(1 - \frac{\epsilon_2}{3 - \epsilon_1}\right),$$
$$g(\epsilon_n) = -\frac{\epsilon_2}{2}\left(f(\epsilon_n) + \frac{1}{2}\epsilon_2 + \epsilon_3\right). \tag{2.3.45}$$

40

In their gauge choice, from the two-point function

$$\langle \zeta^2 \rangle = \frac{1}{2M_{\text{Pl}}^2} \frac{\langle \delta\phi^2 \rangle}{\epsilon_1}, \qquad (2.3.46)$$

we can compute the power spectrum as

$$
\begin{aligned}
\mathcal{P}_\zeta &= \frac{\mathrm{d}\langle \zeta^2 \rangle}{\mathrm{d}\ln k} \\
&= \frac{1}{1-\epsilon_1} \frac{\mathrm{d}\langle \zeta^2 \rangle}{\mathrm{d}N_e} \\
&= \frac{1}{1-\epsilon_1} \frac{1}{2M_{\text{Pl}}^2 \epsilon_1} \left(\frac{\mathrm{d}\langle \delta\phi^2 \rangle}{\mathrm{d}N_e} - \epsilon_2 \langle \delta\phi^2 \rangle \right).
\end{aligned}
\qquad (2.3.47)
$$

We can now use (2.3.44) to write the power spectrum as

$$\mathcal{P}_\zeta = \frac{1}{1-\epsilon_1} \frac{1}{2M_{\text{Pl}}^2 \epsilon_1} \left(\Xi_{\phi\phi} - 2\langle \delta\phi\delta\pi \rangle - \epsilon_2 \langle \delta\phi^2 \rangle \right), \qquad (2.3.48)$$

where

$$\langle \delta\phi\delta\pi \rangle = \frac{fg}{f^2+g} + \frac{1}{2(f^2+g)} \left[\frac{\mathrm{d}\langle \delta\pi^2 \rangle}{\mathrm{d}N_e} - \Xi_{\pi\pi} - 2f \left(\frac{\mathrm{d}\langle \delta\phi\delta\pi \rangle}{\mathrm{d}N_e} - \Xi_{\phi\pi} \right) \right]. \qquad (2.3.49)$$

The function f and g were defined in (2.3.45).

We can check that this expression yields the usual result when we expand it in slow-roll parameters at leading order. In this limit we have $f \simeq 3$ and $g \simeq -3\epsilon_2/2$, which in turn means that $\langle \delta\phi\delta\pi \rangle \simeq -\epsilon_2/2$. Plugging these values in we recover the usual power spectrum

$$\mathcal{P}_\zeta \simeq \frac{1}{2M_{\text{Pl}}^2 \epsilon_1} \Xi_{\phi\phi}. \qquad (2.3.50)$$

This value can also be obtained if the quantum fluctuations $\langle \delta\phi^2 \rangle$ and $\langle \delta\phi\delta\pi \rangle$ are small, meaning the contribution of the $-2\langle \delta\phi\delta\pi \rangle - \epsilon_2 \langle \delta\phi^2 \rangle$ term is negligible when compared to $\Xi_{\phi\phi}$ in (2.3.48). However, short wavelength fluctuations may cause a peak in the noise amplitude. Taking this into account, they predict the power spectrum should approximately be given by

$$\mathcal{P}_\zeta \simeq \frac{1}{2M_{\text{Pl}}^2 \epsilon_1} (\Xi_{\phi\phi} - c\epsilon_2), \qquad (2.3.51)$$

where $c \simeq \langle \delta\phi^2 \rangle$ is a constant. The second term causes a spike in the power spectrum of about 3 orders of magnitude as depicted in figure 2.3.
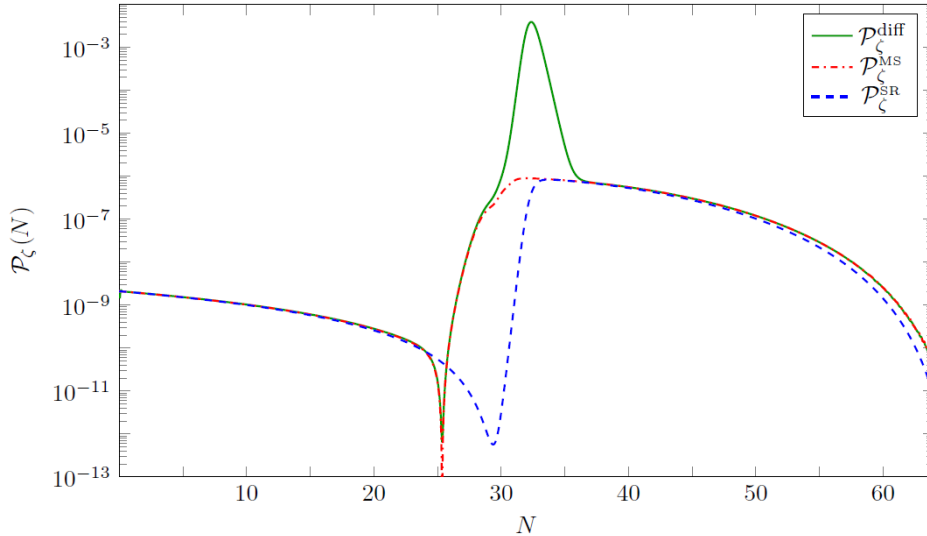
Figure 2.3: Power spectrum $\mathcal{P}_\zeta$ for the curvature perturbations computed from quantum diffusion (green), from the Mukhanov-Sasaki equation (red) and from slow-roll (blue). This picture was taken from [12].

2.3.3 Ultra slow-roll noise

In the following section we will review the final paper [13]. This paper reaches a conclusion at odds with both [11] and [12]. Here we will follow their analysis to better understand their claim.

They begin by considering small quantum fluctuations from classical trajectories in the framework of stochastic single field inflation. We will use the spatially flat gauge, where the scalar field ϕ is split into a background value $\phi_0(\tau)$ and a fluctuation $\delta\phi(\tau, \vec{x})$, while scalar metric fluctuations vanish. The action describing such a system is

$$S = \int \mathcal{L} d\tau d^3 x = \frac{1}{2} \int \left(v'^2 + v\Delta v + \frac{z''}{z} v^2 \right) d\tau d^2 x, \qquad (2.3.52)$$

where $'$ denotes derivation with respect to conformal time τ, $\Delta = \sum_i \partial_i^2$ and

$$v = a\delta\phi, \qquad z = \frac{a\phi_0'}{\mathcal{H}}, \qquad \mathcal{H} = aH. \qquad (2.3.53)$$

Let us remind the definitions of the slow-roll parameters in conformal time

$$\epsilon_1 = -\frac{H'}{aH^2}, \qquad \epsilon_2 = \frac{\epsilon_1'}{\mathcal{H}\epsilon_1}, \qquad \epsilon_3 = \frac{\epsilon_2'}{\mathcal{H}\epsilon_2}. \qquad (2.3.54)$$

42

Taking the conformal time derivative of the Friedmann equation (1.2.3) yields the constraint

$$\frac{H'}{a} = -\frac{\phi_0'^2}{2M_{\rm Pl}^2 a^2}. \tag{2.3.55}$$

Using (2.3.54) and (2.3.55) we find

$$\epsilon_1 = \frac{\phi_0'^2}{2\mathcal{H}^2 M_{\rm Pl}^2}, \tag{2.3.56}$$

which in turn leads us to

$$z = a\sqrt{2\epsilon_1} M_{\rm Pl}. \tag{2.3.57}$$

At this point, we can find an expression for the term z''/z in (2.3.52) in terms of the slow-roll parameters, which reads

$$\frac{z''}{z} = \mathcal{H}^2 \left(2 - \epsilon_1 + \frac{3}{2}\epsilon_2 - \frac{1}{2}\epsilon_1\epsilon_2 + \frac{1}{4}\epsilon_2^2 + \frac{1}{2}\epsilon_2\epsilon_3 \right). \tag{2.3.58}$$

Let us now approximate this expression in a slow-roll background. In slow-roll one has $\epsilon_{i+1} \ll \epsilon_i \ll 1$, therefore

$$\frac{z''_{\rm SR}}{z_{\rm SR}} = \mathcal{H}^2(2 - \epsilon_1 + \mathcal{O}(\epsilon_1^2)). \tag{2.3.59}$$

On the other hand, in ultra slow-roll, the equation of motion (2.3.2) reads

$$\phi_{0,N_e N_e} + (3 - \epsilon_1)\phi_{0,N_e} \simeq 0, \tag{2.3.60}$$

solved by $\phi_{0,N_e} \propto e^{-3N_e}/H$. Therefore, since $\epsilon_1 = \phi_{0,N_e}^2/(2M_{\rm Pl}^2)$ (recall $\mathrm{d}N_e = H\,\mathrm{d}t = \mathcal{H}\,\mathrm{d}\tau$), we have

$$\epsilon_1^{\rm USR} \propto \frac{e^{-6N_e}}{2M_{\rm Pl}^2 H^2}. \tag{2.3.61}$$

We can express higher order slow-roll parameters in terms of the first two. Indeed, we have

$$\epsilon_2^{\rm USR} = \frac{\mathrm{d}}{\mathrm{d}N_e} \ln \epsilon_1^{\rm USR} = -6 + 2\epsilon_1^{\rm USR},$$
$$\epsilon_3^{\rm USR} = \frac{\mathrm{d}}{\mathrm{d}N_e} \ln \epsilon_2^{\rm USR} = 2\epsilon_1^{\rm USR}, \tag{2.3.62}$$
$$\epsilon_4^{\rm USR} = \frac{\mathrm{d}}{\mathrm{d}N_e} \ln \epsilon_3^{\rm USR} = \epsilon_2^{\rm USR},$$

43

and so on. These equations tell us that $\epsilon_n^{\text{USR}} = -6 + 2\epsilon_1^{\text{USR}}$ when n is even, and $\epsilon_n^{\text{USR}} = 2\epsilon_1^{\text{USR}}$ when n is odd. Finally, this means that the z''/z term in ultra slow-roll is given by

$$\frac{z''_{\text{USR}}}{z_{\text{USR}}} = \mathcal{H}^2 \left[2 - 7\epsilon_1^{\text{USR}} + \mathcal{O}\left(\left(\epsilon_1^{\text{USR}}\right)^2 \right) \right]. \tag{2.3.63}$$

We immediately notice that $z''_{\text{SR}}/z_{\text{SR}}$ and $z''_{\text{USR}}/z_{\text{USR}}$ already differ at first order in ϵ_1.

We can now turn our attention to solving the Mukhanov-Sasaki equation

$$\tau^2 \frac{\partial^2 s(\tau, k)}{\partial \tau^2} + \tau \frac{\partial s(\tau, k)}{\partial \tau} + \left(k^2 \tau^2 - \nu^2 \right) s(\tau, k) = 0, \tag{2.3.64}$$

obtained from the action (2.3.52), where

$$\nu^2 = \frac{1}{4} + \frac{z''}{z}\tau^2. \tag{2.3.65}$$

This equation is exactly (2.2.39) written in cosmic time, which is solved by (2.2.48) for constant ν. The authors of [13] fix Bunch-Davies conditions, and find a solution

$$\phi_k(\tau) = \frac{\sqrt{-\tau}}{a} \sqrt{\frac{\pi}{4}} H_\nu^{(2)}(-k\tau), \tag{2.3.66}$$

which is similar to (2.2.50).

At this point, we simply need to apply the formalism of section 2.2, splitting the field and its momentum in a coarse-grained part and a quantum part. In their analysis, they find that the two-point function of the noises is similar to that of the de Sitter approximation (2.2.46), and are given by

$$\langle \xi_1(N_1)\xi_1(N_2) \rangle \simeq \left(\frac{H}{2\pi} \right)^2 \delta(N_1 - N_2), \tag{2.3.67}$$

$$\langle \xi_2(N_1)\xi_1(N_2) \rangle \simeq 0, \tag{2.3.68}$$

$$\langle \xi_2(N_1)\xi_2(N_2) \rangle \simeq 0. \tag{2.3.69}$$

If we take the noise amplitudes to be $\xi_1 = [H/(2\pi)]\xi$ and $\xi_2 = 0$, then

$$\langle \xi(N)\xi(N') \rangle = \delta(N - N'), \tag{2.3.70}$$

where the equation of motion for the quantum part ϕ_Q in real space is given by

$$\phi_{Q,N_e N_e} + 3\phi_{Q,N_e} = \frac{3H}{2\pi}\xi(N). \tag{2.3.71}$$

We can now integrate this equation and find that, with suitable initial conditions, the curvature perturbations in real space is given by

$$\delta\phi_Q(N) = \phi_Q(N) - \langle \phi_Q(N) \rangle = \int_0^N dN_2 \, e^{-3N_2} \int_0^{N_2} dN_1 \, \frac{3H}{2\pi} e^{3N_1} \xi(N_1). \tag{2.3.72}$$

44

Since we are interested in the noise auto-correlation, using (2.3.70) we find that

$$\langle \delta\phi_{\mathrm{Q}}(N)\delta\phi_{\mathrm{Q}}(N)\rangle = \frac{H^2}{4\pi^2}\left(N - \frac{1}{2} - \frac{e^{-6N}}{6} + \frac{2e^{-3N}}{3}\right)$$
$$\simeq \frac{H^2}{4\pi^2}\left(N - \frac{1}{2}\right). \qquad (2.3.73)$$

We have neglected the decaying modes since we are only interested in the behaviour at leading order. The linear growth in N is motivated by the fact that we are carrying out our calculations in real space. We can find the power spectrum by turning to Fourier space:

$$\mathcal{P}_{\delta\phi} \simeq \frac{\mathrm{d}}{\mathrm{d}N}\langle \delta\phi_{\mathrm{Q}}(N)\delta\phi_{\mathrm{Q}}(N)\rangle = \frac{H^2}{4\pi^2}\left(1 + \mathcal{O}\big(\epsilon_1^{\mathrm{USR}}\big)\right). \qquad (2.3.74)$$

2.3.4 Summary

In this section we will comment on the results found by the three papers summarised in the sections above. A conclusive view on the role of quantum stochastic effects on ultra slow-roll backgrounds and its impact on the production of primordial black holes is still a subject of active research, to which we present our contribution in section 3.

The authors of the paper [11] conclude that quantum diffusion should play a central role in the quantitative analysis of PBH formation in single field inflation. They assumed the diffusion coefficient to be of zero-th order in slow-roll parameters. Indeed, they defined $D = 9H^2/(4\pi^2)$.

This quantity is directly related to the matrix (2.2.46). As one can easily see, the physical limit $\sigma \to 0$ does lead to the simple definition employed by [11] when the background field evolves in a perfectly de Sitter space ($\nu = 3/2$). However, any slight variation from this value will cause the matrix (2.2.46) to show an unavoidable dependence on the time variable σ, as seen in (2.2.52), (2.2.53) and (2.2.54).

This means that the diffusion matrix D features more than one degree of freedom, forcing the introduction of more than one random Gaussian noise with potentially time-dependent amplitudes. For example, even in de Sitter space, keeping terms up to order two in (2.2.46) will modify the diffusion coefficient $D_{\phi\phi}$ and introduce quantum noise in the field-momentum direction. For this reason, choosing a more precise diffusion coefficient might be necessary.

The authors of [12] reach the conclusion that, in agreement with [11], quantum diffusion effects do play a significant role in the production of PBHs during USR. However unlike [11] they claim that the power spectrum during this phase receives a huge enhancement due to the two-point correlation function $\langle \delta\phi^2 \rangle$.

This enhancement is achieved by evaluating the curvature perturbations at different times for different modes to construct the power spectrum (2.3.51). Scales that leave

the horizon deep in USR have their slow-roll parameters ϵ and η evaluated after the transition took place, in apparent violation of causality.

The authors of [13] follow an analysis which is similar to that of [12], in the sense that they evaluate the power spectrum through a two-point correlation function. However, the respective results are in disagreement with each other, since [13] finds no enhancement of quantum diffusion. They claim the reason why [12] found an incorrect result lies in the assumption that, at super-horizon scales, the growing and decaying modes are to be discarded (see the discussion leading to (2.3.36)). They instead claim that curvature perturbations at such scales cannot be considered constant during an ultra slow-roll phase, being dominated by the growing mode.

Furthermore, they mention their disagreement with [11] about the role of quantum diffusion effects in PBH abundance stems from their different views on the nature of the power spectrum. They claim [11] had no right to promote it to a stochastic variable, since it is already a mediated quantity, being an expectation value.

In their estimates of the noise two-point function, the authors of [13] neglect the fact that the background is undergoing a rapid transition which, as we will show, leads to a different noise amplitude.

Chapter 3

The effects of sudden transitions on the stochastic noise amplitude

In this chapter we will mainly focus on the determination of the properties of the Gaussian random noise, in particular its two-point function given that the aim of this work is to clarify the role of quantum diffusion effects on the abundance of primordial black holes, since there is no general agreement in the literature as to whether or not these effects should play a significant role.

We will primarily do our calculations with the Starobinsky potential, while occasionally switching to a simpler de Sitter model or to a more realistic potential described in appendix B. We have made this choice due to the fact that Starobinsky potential remains simple enough while still capturing the main qualitative features required to induce an USR phase: two slow-roll flat regions with hierarchical slopes.

The vast majority of calculations are carried out using Wolfram Mathematica, often shortened to Mathematica. This extremely versatile computing system based on the Wolfram Language programming language was first released on June 23, 1988 by Wolfram Research. The version used in this work is version 11.3, released on March 8, 2018. We chose to adopt this particular language because it complements symbolic programming while still providing the user with many advanced instruments of numerical analysis.

3.1   Potentials and parameter choice

Choosing the appropriate potential to correctly reproduce experimental results is often a difficult task. However, sometimes a simple potential is enough to capture the main features of a particular phenomenon. In this section we will present the potentials we based our analysis on.

3.1.1 De Sitter potential

A Universe where the potential of the field driving inflation is a constant is called a de Sitter Universe. In such a situation, the accelerated expansion ($\ddot{a} > 0$) will go on forever, since the field will keep evolving in a constant background without ever finding a stable minimum. This is clearly not a realistic case, since in the early Universe inflation must come to an end at some point. To achieve this, we can manually stop inflation after we have let the field evolve for some time.

In our analysis, we used the constant potential

$$V(\phi) = 10^{-2}. \tag{3.1.1}$$

Inflation starts at $N_e = 0$ number of e-foldings and decided to stop integration at $N_{\mathrm{end}} = 70$. This particular value was chosen because, in order to solve the Big Bang problems, we need to have a inflationary period which lasts $\gtrsim 60$. Furthermore, more realistic models such as the one in appendix B suggest this period should indeed last ~ 70.

The initial value for the inflaton field was taken to be $\phi(0) = \phi_0 = 0$. Since the theory is shift invariant, any initial value should not matter when calculating observables. The velocity of the field was set to $\partial\phi/\partial N_e\big|_{N_e=0} = 0$. This value does not play any significant role anyway since any initial velocity that the field might have before observable inflation begins will get exponentially suppressed shortly thereafter.

Given the simplicity of this model, it cannot give rise to any realistic effects found in other potentials. Nevertheless, this potential is useful from a pedagogical point of view since it reproduces many of the features of inflation. This potential is useful as a consistency check of the numerical procedure given that we have the analytical results for the noise correlators (2.2.46).

3.1.2 Starobinsky model

This is the main potential we used in this work. It was introduced in 1992 by Russian astrophysicist Starobinsky [17]. We already introduced this potential in section 2.3.1, but we will repeat here for convenience's sake. The potential is given by

$$V(\phi) = V_0\left[1 + \frac{1}{2}\left(\sqrt{2\epsilon_+} - \sqrt{2\epsilon_-}\right)(\phi - \phi_{\mathrm{c}})\tanh\left(\frac{\phi - \phi_{\mathrm{c}}}{\delta}\right) \right. \\ \left. + \frac{1}{2}\left(\sqrt{2\epsilon_+} + \sqrt{2\epsilon_-}\right)(\phi - \phi_{\mathrm{c}})\right]. \tag{3.1.2}$$

As specified in section 2.3.1, this is not the form Starobinsky wrote his potential in, but rather a particular parametrisation found in [11].

The normalisation value was chosen to be $V_0 = 1$. The two parameters ϵ_- and ϵ_+ (recall they are the slow-roll parameters before and after the transition) need to be $\ll 1$
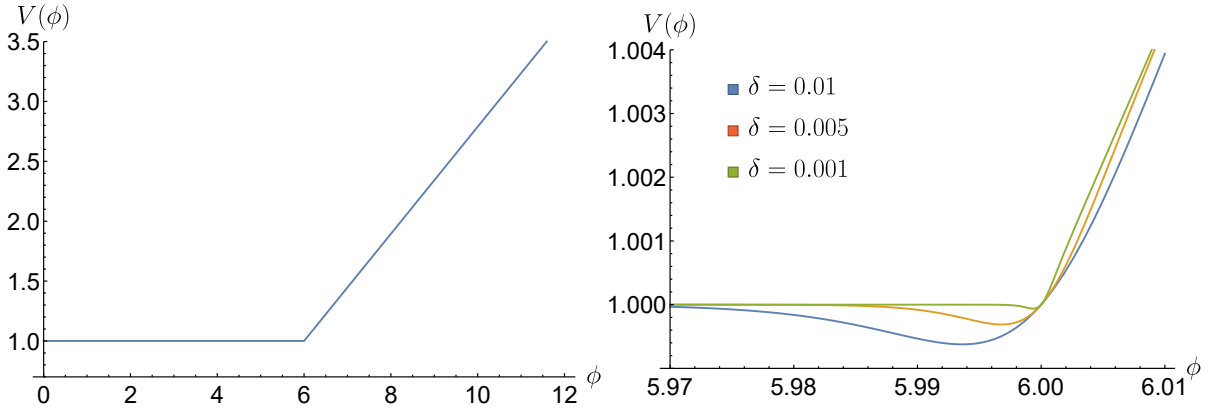
Figure 3.1: Starobinsky potential with the parametrisation by [11]. The right panel represents the three choices $\delta = 0.01$ (blue), $\delta = 0.005$ (orange) and $\delta = 0.001$ (green).

if we want slow-roll to hold both before and after the transition. In order to induce USR dynamics, we need to take $\epsilon_- \ll \epsilon_+$. We have chosen $\epsilon_- = 10^{-15}$ and $\epsilon_+ = 10^{-1}$.

Another very meaningful parameter is δ. It is proportional to the duration of the transition USR phase. We chose $\delta = 0.01$ since we found this value to be small enough not to ruin the preceding and succeeding slow-roll phases while giving rise to a phase long enough to allow for a stable numerical analysis.

Once again, we manually stop integration at $N_{\text{end}} = 70$, in analogy with the de Sitter case, and set $\phi(0) = \phi_0 = 0$ and $\partial\phi/\partial N_e\big|_{N_e=0} = 0$ (see section 3.1.1 for an explanation of why this is sensible), with the transition happening at $\phi_c = 6$.

In figure 3.1 we have shown the shape of Starobinsky potential and a magnified version around the transition.

3.1.3 CicoliDiazPedro

We also studied the evolution of the background and the curvature perturbation in a realistic potential, obtained in the framework of type IIB string theory [18], given by

$$V(\phi) = V_0 \left[C_1 - e^{-\frac{1}{\sqrt{3}}\hat{\phi}} \left(1 - \frac{C_6}{1 - C_7 e^{-\frac{1}{\sqrt{3}}\hat{\phi}}} \right) + C_8 e^{\frac{2}{\sqrt{3}}\hat{\phi}} \left(1 - \frac{C_9}{1 + C_{10} e^{\sqrt{3}\hat{\phi}}} \right) \right], \quad (3.1.3)$$

We refer to appendix B for more details on the shape of the potential and for a sketch of how it can be derived.

This potential was mainly used to verify to what extent the behaviour of the inflaton under the influence of simple linear potentials, such as Starobinsky, well approximates the real behaviour under realistic potentials. The shape of this potential is shown in figure 3.2.
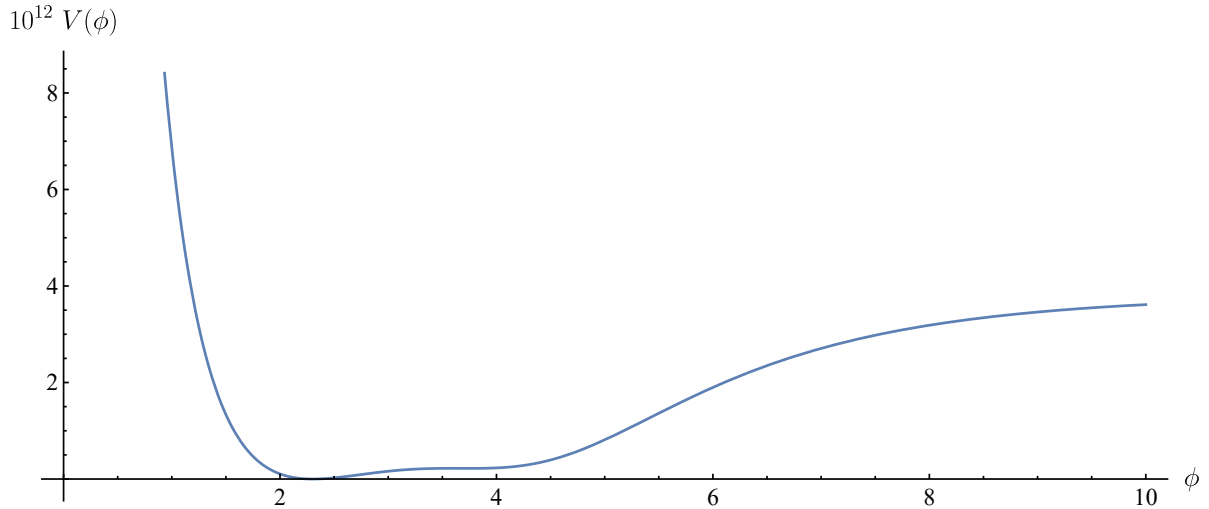
Figure 3.2: Shape of the potential described in appendix B. The plateau around $\phi \sim 3.5$ induces USR dynamics.

3.2 Numerical analysis

In this section we will describe how we integrated the equations of motion to find the solutions. A numerical integration is desired since it greatly reduces the complexity of the analysis, given that they feature two functions of time, i.e. H and ϕ, and their derivatives.

Since we always used the number of e-foldings as our time variable, we will employ $'$ to represent derivation with respect to the number of e-foldings instead of $, N_e$.

3.2.1 Background solution

Since we are dealing with stochastic inflation, we will coarse-grain the scalar field $\phi = \bar{\phi} + \delta\phi$ as usual. The first step of our analysis is finding the solution to the classical unperturbed equation of motion for the coarse-grained scalar inflaton field $\bar{\phi}$. This equation is the usual Klein-Gordon equation (1.4.5) written in number of e-foldings which reads

$$\bar{\phi}'' + (3 - \epsilon)\bar{\phi}' + \frac{V_{,\phi}}{H^2} = 0. \tag{3.2.1}$$

Clearly this equation alone is not enough since $H = H(N_e)$ is a function of time. Its time evolution is provided by the time derivative of the Friedmann equation (1.2.3) given by
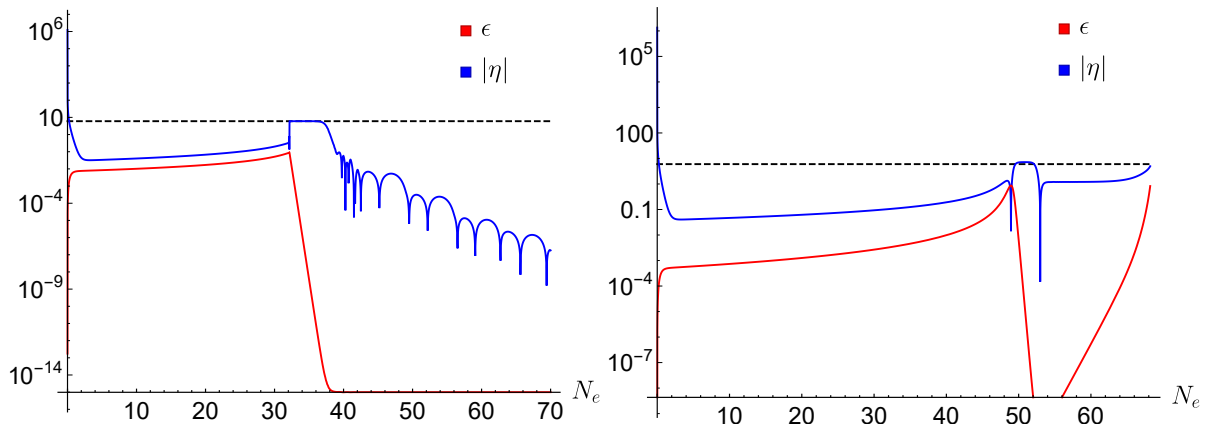
$$H' = -\frac{H\bar{\phi}'^2}{2}. \tag{3.2.2}$$

Figure 3.3: In this graph we have used expressions (3.2.4) and (3.2.5) to plot the shape of the slow-roll parameters ϵ and $|\eta|$ in the Starobinsky model (left panel) and the realistic model from [14] (right panel). The dashed line is drawn at 6, and we can see that $|\eta| \simeq 6$ during USR. Notice that the behaviour of $|\eta|$ at high numbers of e-foldings in the left panel is due to the fact that η oscillates about $\eta \simeq 0$ when the second slow-roll phase is reached.

We can numerically solve (3.2.1) and, at the same time, (3.2.2) to find $\bar{\phi}$ and H as functions of the number of e-foldings. The initial condition on H is given by the Friedman equation (1.2.3) at $N_e = 0$, that is

$$H(0) = H_0 = \left. \sqrt{\frac{V}{3 - \bar{\phi}'^2/2}} \right|_{N_e=0} . \tag{3.2.3}$$

It is useful to point out that the Hubble parameters ϵ, η and κ can be expressed in terms of the fields $\bar{\phi}$ and H. Indeed, from the Friedmann equation (1.2.3) it is easy to find that

$$\epsilon = -\frac{H'}{H} = \frac{\bar{\phi}'^2}{2}, \tag{3.2.4}$$

and, from (3.2.1) and (3.2.4), that

$$\eta = \frac{\epsilon'}{\epsilon} = -6 + 2\epsilon - \frac{2V_{,\phi}}{\bar{\phi}H^2}. \tag{3.2.5}$$

The shape of the slow-roll parameters using such expressions is shown is figure 3.3.

3.2.2 First order perturbation solution

Now that we have obtained the time evolution of the background $\bar{\phi}$, we can move on to the short-wavelength part $\delta\phi$. As we mentioned in section 2.2.4, the Hamiltonian system
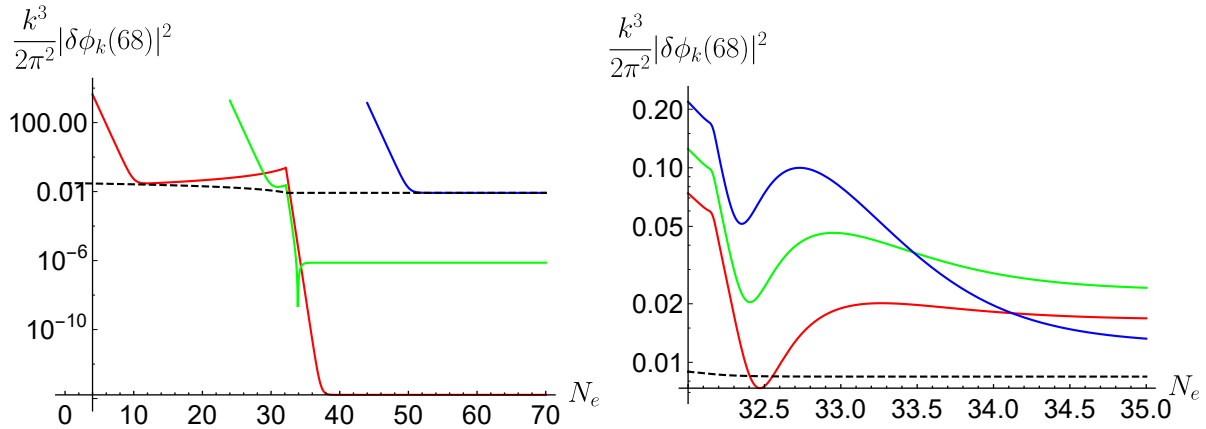
Figure 3.4: Solutions for equation of motion (3.2.6) for six different values of the scale k. In the left panel, we have shown the full evolution of three modes exiting the horizon at 10 (red), 30 (green) and 50 (blue) e-foldings. Notice that as soon as the perturbation enters the horizon, it becomes constant until it reaches the USR transition. In the right panel we have shown the evolution shortly after the transition for modes that leave the horizon at 33.0 (red), 33.3 (green), which undergoes the highest amount of enhancement, and 33.6 (blue) e-foldings.

formed by (2.2.18) and (2.2.19) leads to the equation of motion for ϕ_k

$$\phi_k'' + (3 - \epsilon)\phi_k' + \left[\left(\frac{k}{aH}\right)^2 + \frac{V_{,\phi\phi}}{H^2} + (\bar{\phi}')^2(-3 + \epsilon - \eta)\right]\phi_k = 0, \qquad (3.2.6)$$

written in Fourier space. The extra term $(\bar{\phi}')^2(-3 + \epsilon - \eta)$ in the effective mass appears since ϕ is responsible for the background evolution, i.e. it is not a spectator. We derive this term in appendix A, following [10]. It should be pointed out that the form in which that term has been presented here is different than the one in appendix A. However, using the equation of motion (3.2.1) for the coarse-grained field and (3.2.5), easily leads one to find that the two expressions are equivalent.

In order to achieve numerical stability, we have shifted the value of the number of e-foldings that appears in the scale factor $a = \ln N_e$ by a quantity N_{shift}, i.e. we defined $a = \ln(N_e - N_{\text{shift}})$. This is perfectly valid and does not change the physics since the full definition for the scale factor actually is $a = a_{\text{i}} \ln N_e$. Choosing a value for N_{shift} amounts to choosing a particular a_{i}, which is arbitrary to begin with.

We have taken initial conditions for the quantum field ϕ_k to be of Bunch-Davies type.
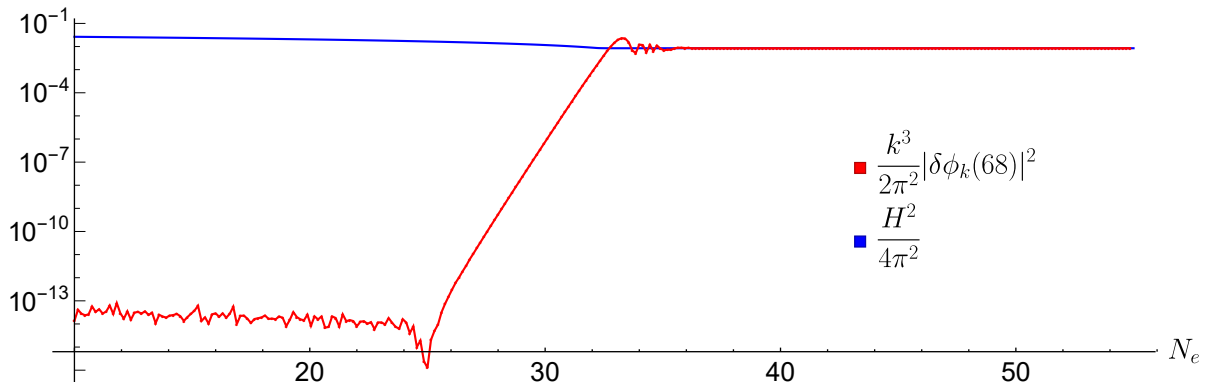
Figure 3.5: Power spectrum in the Starobinsky model in logarithmic scales, as opposed to the linear one of figure 3.6. Notice the super-horizon evolution of scales that leave the horizon after the transition ($N_e \sim 32$).

They read

$$\phi_k(N_{\text{in}}) = \left. \frac{1}{a\sqrt{2k}} \right|_{N_e = N_{\text{in}}}, \tag{3.2.7}$$

$$\phi'_k(N_{\text{in}}) = -\left. \frac{1}{a\sqrt{2k}} \left(1 + \frac{ik}{aH} \right) \right|_{N_e = N_{\text{in}}}, \tag{3.2.8}$$

in Fourier space. These conditions mean that the field is in its vacuum state well before exiting the horizon. The value N_{in} represents the point in time where integration of (3.2.6) begins. Ideally, this value should coincide with the beginning of observable inflation. However, carrying out such an integration would take far too long. Instead, we opted to begin integration at a reasonable number of e-foldings before horizon exit for each mode.

In order to build the power spectrum, we solved the equations of motion (3.2.6) n times, each with a different value for k, and evaluated each solution $\phi_k(N_e)$ at $N_e \simeq N_{\text{end}}$. In figure 3.4 we show the result of our numerical integration for six different values of k. Notice that, as we mentioned, integration starts moments before horizon exit, and not at the very beginning of inflation. However, we can safely disregard this early behaviour for two reasons: firstly we expect a constant slope for the whole duration of the sub-horizon evolution; secondly, we are only interested in late time behaviour, since the power spectrum is constructed from those moments.

As soon as the perturbation exits the horizon, it quickly becomes constant up until it reaches the USR transition. During this phase, the solution is no longer of the Bunch-Davies type, meaning its form is no longer that of (2.2.50). Instead it must feature both a $H_\nu^{(2)}$ and a $H_\nu^{(1)}$ contribution, according to the general solution (2.2.48). Physically, this means that the field is no longer in its ground state, since the transition has raised
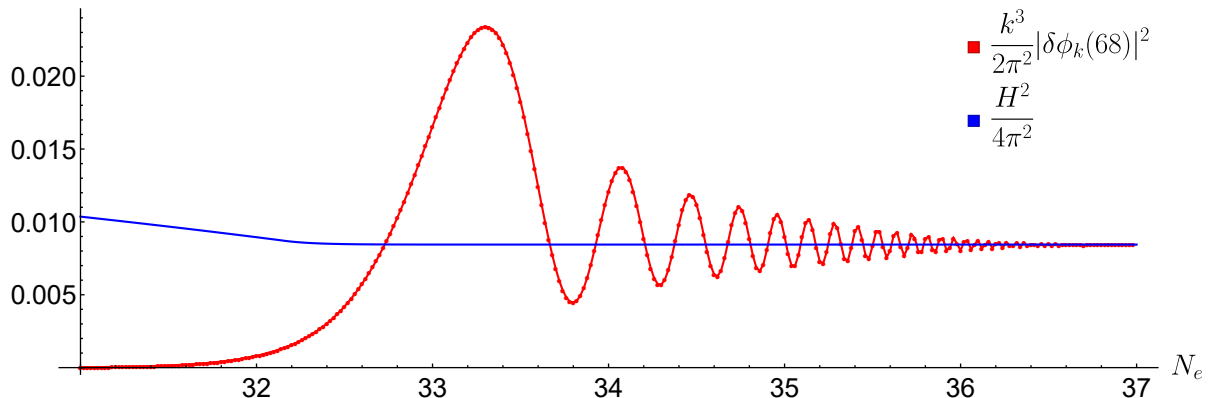
53

Figure 3.6: Power spectrum obtained from the solutions in figure 3.4. It was constructed from $n = 200$ points. In the figure we also show the slow-roll approximation $H^2/(4\pi^2)$. It is clear from the graph that this value is reached after the transition, while before there is strong disagreement.

the field to an excited state. This is a well known feature of time dependent backgrounds, that becomes more important whenever the background undergoes sudden transitions.

Furthermore, the index ν, which is real before the transition, becomes purely imaginary during USR, before going back to being real after slow-roll is restored again. This is not surprising. From definition (2.2.47) we expect $\nu \simeq 3/2$ in slow-roll, since $V_{,\phi\phi} \simeq 0$, while it becomes imaginary when $V_{,\phi\phi} > 9H^2/4$, which is clearly satisfied during USR.

The exact imaginary value taken by ν during USR depends on the particular model and its parameters. It mostly depends on the duration of the USR phase. In particular, shorter USR phases, generated for example by a small δ in Starobinsky, will result in a big $|\eta|$ during USR. For our choices of parameters, we found that typically $|\nu| \sim \mathcal{O}(10)$.

In figure 3.5, we show the power spectrum for the Starobinsky model. In figure 3.6 we show the Starobinsky power spectrum focused on those scales that leave the horizon close to the USR phase.

3.3 Analytical analysis

In order to have an exact check of the numerical results, we also developed an analytical method to treat the same problem. While we can still use the background $\bar{\phi}$ found in section 3.2.1, some approximations must be done on the equation of motion (3.2.6) for the quantum part so that (2.2.48) is still a solution to it.
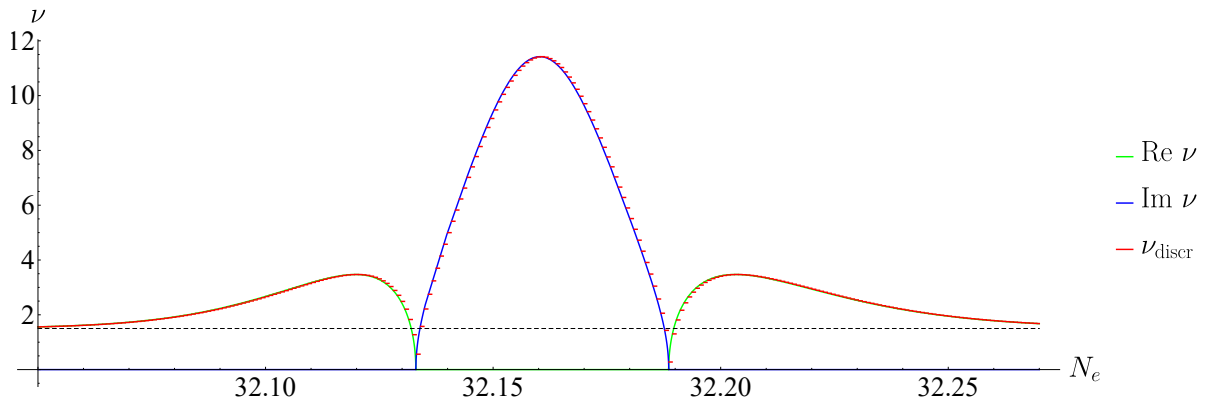
Figure 3.7: In this graph we show the real (green) and imaginary (blue) parts of the index ν for Starobinsky model with the parameters chosen in section 3.1.2. Additionally, we also show the discretised index ν_{discr}. As evident from the picture, ν_{discr} is a collection of successive step theta functions, so that during each sub-interval the index of the Hankel function is constant. The far left and far right parts of ν are not shown since it quickly approaches 3/2 (dashed black).

3.3.1   Discretisation of the index ν

Since the Hubble parameter does not change much during inflation, we considered it to be constant in our analytical calculations. Therefore, in this section, the symbol H refers to the Hubble parameter evaluated towards the end of inflation, i.e. $H = H(N_{\text{end}})$. For this reason, we also set $\epsilon = 0$. Thus, the equation of motion is given by

$$\phi_k'' + 3\phi_k' + \left[\frac{9 - 4\nu^2}{4} + \left(\frac{k}{aH} \right)^2 \right] \phi_k = 0, \qquad (3.3.1)$$

where ν was defined in (2.2.47).

   If we want (2.2.48) to be a valid solution to the equation of motion (3.3.1), the index ν needs to be a constant. However, as we explained in section 3.2.2, ν dramatically changes when approaching USR. In order to overcome this, we divided the interval of integration into multiple sub-intervals, each with constant ν [19]. Then, one only needs to link together the solutions by imposing continuity conditions on the perturbation ϕ_k and its derivative ϕ_k'.

   For instance, say the i-th transition involves a change from ν_i to ν_{i+1}. The solution to (3.3.1) before the transition is given by

$$\phi_k = \left(\frac{k}{aH} \right)^{3/2} \left[\alpha_i H_{\nu_i}^{(1)} \left(\frac{k}{aH} \right) + \beta_i H_{\nu_i}^{(2)} \left(\frac{k}{aH} \right) \right]. \qquad (3.3.2)$$
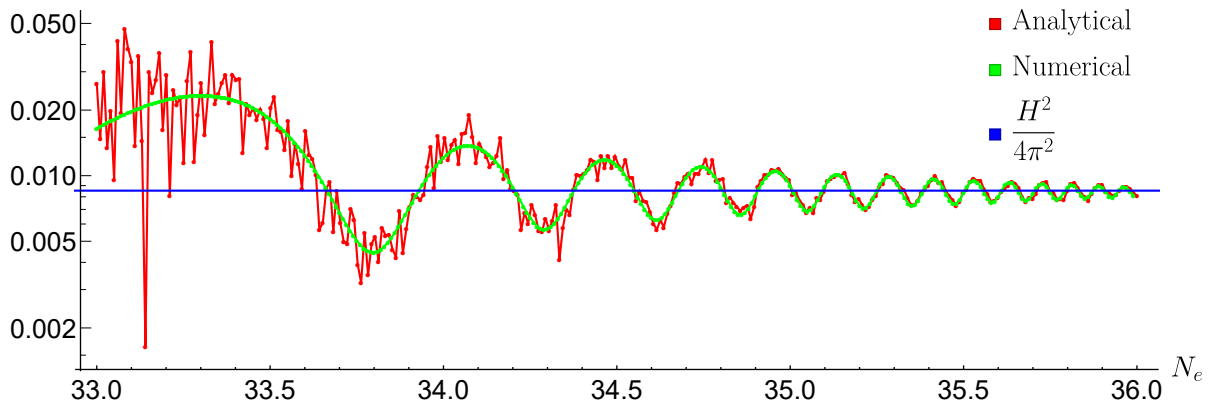
55

Figure 3.8: Power spectrum in Starobinsky with the analytical (red) method. There is good agreement between the two methods employed in this work.

After the transition, the solution does not change in form: (3.3.2) is still a solution to (3.3.1) provided we carry out the substitutions $\nu_i \mapsto \nu_{i+1}$, $\alpha_i \mapsto \alpha_{i+1}$ and $\beta_i \mapsto \beta_{i+1}$. The two coefficients can be found through continuity conditions to be given by

$$
\begin{aligned}
\alpha_{i+1} = {} & \alpha_i \frac{(H^{(1)}_{\nu_i-1} - H^{(1)}_{\nu_i+1})H^{(2)}_{\nu_{i+1}} + H^{(1)}_{\nu_i}(H^{(2)}_{\nu_{i+1}+1} - H^{(2)}_{\nu_{i+1}-1})}{(H^{(1)}_{\nu_{i+1}-1} - H^{(1)}_{\nu_{i+1}+1})H^{(2)}_{\nu_{i+1}} + H^{(1)}_{\nu_{i+1}}(H^{(2)}_{\nu_{i+1}+1} - H^{(2)}_{\nu_{i+1}-1})} \\
& + \beta_i \frac{(H^{(2)}_{\nu_i-1} - H^{(2)}_{\nu_i+1})H^{(2)}_{\nu_{i+1}} + H^{(2)}_{\nu_i}(H^{(2)}_{\nu_{i+1}+1} - H^{(2)}_{\nu_{i+1}-1})}{(H^{(1)}_{\nu_{i+1}-1} - H^{(1)}_{\nu_{i+1}+1})H^{(2)}_{\nu_{i+1}} + H^{(1)}_{\nu_{i+1}}(H^{(2)}_{\nu_{i+1}+1} - H^{(2)}_{\nu_{i+1}-1})}, \\
\beta_{i+1} = {} & \alpha_i \frac{(H^{(1)}_{\nu_i-1} - H^{(1)}_{\nu_i+1})H^{(1)}_{\nu_{i+1}} + H^{(1)}_{\nu_i}(H^{(1)}_{\nu_{i+1}+1} - H^{(1)}_{\nu_{i+1}-1})}{(H^{(1)}_{\nu_{i+1}+1} - H^{(1)}_{\nu_{i+1}-1})H^{(2)}_{\nu_{i+1}} + H^{(1)}_{\nu_{i+1}}(H^{(2)}_{\nu_{i+1}-1} - H^{(2)}_{\nu_{i+1}+1})} \\
& + \beta_i \frac{(H^{(2)}_{\nu_i-1} - H^{(2)}_{\nu_i+1})H^{(1)}_{\nu_{i+1}} + H^{(2)}_{\nu_i}(H^{(1)}_{\nu_{i+1}+1} - H^{(1)}_{\nu_{i+1}-1})}{(H^{(1)}_{\nu_{i+1}+1} - H^{(1)}_{\nu_{i+1}-1})H^{(2)}_{\nu_{i+1}} + H^{(1)}_{\nu_{i+1}}(H^{(2)}_{\nu_{i+1}-1} - H^{(2)}_{\nu_{i+1}+1})}.
\end{aligned}
\tag{3.3.3}
$$

The argument of each Hankel function is always $k/(aH)$, and it was omitted for clarity.

We can repeat (3.3.3) n times, once for each transition. The final coefficients are the ones that determine the final solution.

A part of the Mathematica program was devoted to the discretisation of the index $\nu(N_e)$. The result is shown in figure 3.7. In that figure, the model used to find the shape of the function $\nu(N_e)$ is Starobinsky. We can see that for numbers of e-foldings $N_e < 32$, the index is very close to $3/2$. This is because the field is in almost perfect slow-roll. When the transition is approached, ν starts to increase, then plummets to zero and becomes imaginary. Its imaginary part reaches a peak of $\sim 11i$ at $N_e \sim 32.16$ numbers of e-foldings, then a symmetric behaviour is observed, and for $N_e > 32.3$ the index is again $3/2$. This is because in Starobinsky models, the phase after the transition

56

is slow-roll. However, the coefficient α responsible for the $H_\nu^{(1)}$ contribution is different from zero after the transition. This means that, while the field propagates in a de Sitter background, it is in an excited state due to the transition.

When the duration of the transition (in picture 3.7 we can see that it lasts ~ 0.3 e-foldings) is increased, for instance by increasing the value of the parameter δ in(3.1.2), the maximum value of Im ν decreases. In the limit $\delta \to \infty$, the transition disappears since the potential is linear with only one slow-roll phase. This can be checked by considering the limit of (3.1.2) for $\delta \to \infty$, which reads

$$V(\phi) = V_0 \left[1 + \frac{1}{2} \left(\sqrt{2\epsilon_+} + \sqrt{2\epsilon_-} \right) (\phi - \phi_c) \right] + \mathcal{O}\left(\delta^{-1} \right). \qquad (3.3.4)$$

We used the discretisation method illustrated in figure 3.7 to find the power spectrum through analytical solutions to (3.3.1). The resulting power spectrum is shown in figure 3.8 and, apart from some noise, the analytical solution has the same shape of the purely numerical one.

3.4   Conclusions

In the present work we focused on the effects of sudden transitions on the amplitude of the stochastic noise in a Starobinsky potential and their impact on the production of primordial black holes in single field inflation by checking whether or not the power spectrum undergoes sufficient enhancement. Firstly, in chapter 1, we introduced the main ideas that are utilised to build the foundations of modern cosmology, such as the cosmological principle, general relativity, the Friedmann equations and, lastly, the Hot Big Bang theory with its problems and solutions.

Then, in chapter 2, we showed how primordial black holes can be responsible for a significant fraction of the dark matter abundance today in the Universe given current observational constraints and investigated the main mechanism that allows for the creation of such objects: an enhancement in the primordial power spectrum due to non-negligible quantum effects that amplify the two-point correlation function of the stochastic noise. In section 2.2, we followed the Hamiltonian formalism developed in [10] and summarised the main ideas of coarse-graining of the quantum field ϕ and its momentum π that allow for a separate treatment of the time-dependent background and the space-time-dependent quantum fluctuations.

However, in the current literature, one can find multiple works that apply this very same formalism, but find results that are incompatible with each other. We summarised three of those article, namely [11, 12, 13], in section 2.3 and presented their findings, commenting on the respective claims in section 2.3.4.

Chapter 3 is dedicated to our analysis and contribution on the impact of stochastic effects on the power spectrum enhancement in a Starobinsky potential. First of all, we

checked that this potential leads to a dynamics similar to that of a more realistic model and found a qualitatively similar behaviour in the slow-roll parameters, as depicted in figure 3.3. Although this potential is relatively simple, it is rich enough to allow for the introduction of an ultra slow-roll phase in the dynamics of the scalar field ϕ during inflation. This causes the field to undergo a sudden transition when approaching the USR regime, which can be observed in the dramatic change of the Hankel function index ν depicted in figure 3.7. As a result, the field is excited from its ground state (achieved by imposition of Bunch-Davies conditions at the beginning of observable inflation) to an excited state. This is a known effect, but its implications are still under scrutiny.

We have implemented both a numerical and an analytical procedure that allows for the construction of the noise amplitude for different scales. As one can see from figure 3.5, small scales have their noise amplitude suppressed to values much smaller than the Hubble scale squared, whereas modes that leave the horizon near and after the transition undergo a rapid growth until they reach the constant value (after some oscillation visualised in figure 3.6) of $H^2/(4\pi^2)$. The good agreement between the analytical and numerical methods in shown in figure 3.8.

With this computation we demonstrate that, for the Starobinsky potential, the estimates of the noise amplitude found in the literature miss important physics. It would be interesting to compare our findings regarding the noise amplitude for the Starobinsky model with some more realistic ones, and to be able to quantify its effects on the primordial black hole abundance. We leave these issues for future work.

Appendix A

Coupling the inflaton to metric fluctuations

In (3.2.6) we introduced a term in the equation of motion for the scalar perturbations which is proportional to the velocity of the background field. This term was ignored then because of its small contribution in simple potentials, but it plays an important role if the inflaton is strongly coupled to the metric. This term takes into account the back-reaction of the scalar perturbations on the metric itself. Indeed, scalar perturbations are expected to modify the metric just like any other form of energy. In this appendix we will work out how that term can be obtained. Let us use a spatially-flat gauge, where the metric reads

$$\mathrm{d}s^2 = -N(\tau)^2[1 + 2A(\tau, \vec{x})]\,\mathrm{d}\tau^2 + 2a^2\partial_i B(\tau, \vec{x})\,\mathrm{d}\tau\,\mathrm{d}x^i + a^2\delta_{ij}\,\mathrm{d}x^i\,\mathrm{d}x^j\,, \qquad (A.1)$$

where $A \ll 1$ and $B \ll 1$ are small perturbations from the spatially-flat metric (2.2.12). The same formalism from section 2.2 can be applied. A metric such as (A.1) will result in the same Hamilton equations (2.2.10) and (2.2.11) for the uncoupled case, provided the lapse function is remapped as $N(\tau, \vec{x}) \mapsto N(\tau)[1 + A(\tau, \vec{x})]$ and the shift vector as $N^i(\tau, \vec{x}) \mapsto \partial^i B(\tau, \vec{x})$. We will drop the τ and $\vec{x}$ dependencies from now on for brevity's sake. When this substitution is carried out, the resulting Hamilton equations are

$$\dot{\phi} = \frac{N}{a^3}\pi_\phi(1 + A) + \partial^i B \partial_i \phi, \qquad (A.2)$$

$$\dot{\pi}_\phi = -Na^3 V_{,\phi}(1 + A) + Na[\Delta\phi + \partial^i(A\partial_i\phi)] + \partial_i[(\partial^i B)\pi_\phi]. \qquad (A.3)$$

At this point, following the procedure of section 2.2.2, one needs to pick a cut-off wavelength $k_\sigma(\tau)$ and split each field in a coarse-grained field $(\bar{\phi}, \bar{\pi})$ and its quantum fluctuations $(\phi_{\mathrm{Q}}, \pi_{\mathrm{Q}})$ through the use of a window function $W(k/k_\sigma)$ (see equations (2.2.16) and (2.2.17) for reference).

In theory, the same coarse-graining treatment should also be applied to the functions which describe metric fluctuations, namely $A = \bar{A} + A_{\mathrm{Q}}$ and $B = \bar{B} + B_{\mathrm{Q}}$, with

$$A_{\mathrm{Q}} = \int_{\mathbb{R}^3} \frac{\mathrm{d}^3 k}{(2\pi)^{3/2}} W\left(\frac{k}{k_\sigma}\right) \left[a_k A_k(\tau) e^{-i\vec{k}\cdot\vec{x}} + a_k^\dagger A_k^\star(\tau) e^{i\vec{k}\cdot\vec{x}}\right], \tag{A.4}$$

and similarly for B. However, the coarse-grained parts $\bar{A}$ and $\bar{B}$ can be set to vanish. Let us now go over three reasons why this can be done.

Firstly, since the lapse and shift functions are pure gauge choices, their classical value should not matter and can be reabsorbed into the definition of N and a^2.

Secondly, the line element (A.1) has been written in such a way that two sectors clearly appear: in that expression, we have two quantities which only depend on the time variable τ (namely N and a^2) and two more which additionally depend on the point in space $\vec{x}$ (namely A and B). The first group of variables is part of a homogeneous and isotropic vector, since their value is constant throughout space. The second group forms the inhomogeneous and perturbative sector. Therefore, there is no reason to introduce further homogeneous degrees of freedom ($\bar{A}$ and $\bar{B}$ would be functions of time only) in the inhomogeneous sector.

Thirdly, at large scales (small k) the scalar field is approximately its coarse-grained part, i.e. $\phi \simeq \bar{\phi}$. Since this field is constant in space, its metric should be too, hence it cannot generate any perturbation in the metric.

Let us now linearise equations (A.2) and (A.3) by throwing away any term with at least two quantum parts. Given the reasons above, we can safely assume $\bar{A} = \bar{B} = 0$. This leads us to the result

$$\dot{\bar{\phi}} + \dot{\phi}_{\mathrm{Q}} = \frac{N}{a^3} \left[\bar{\pi}\left(1 + A_{\mathrm{Q}}\right) + \pi_{\mathrm{Q}}\right], \tag{A.5}$$

$$\dot{\bar{\pi}} + \dot{\pi}_{\mathrm{Q}} = Na\Delta\phi_{\mathrm{Q}} - Na^3 \left[V_{,\phi}\left(1 + A_{\mathrm{Q}}\right) + V_{,\phi\phi}\phi_{\mathrm{Q}}\right] + \bar{\pi}\square B_{\mathrm{Q}}. \tag{A.6}$$

It must be noted that this expression was obtained by expanding the potential $V_{,\phi}(\phi)$ about the coarse-grained value $\bar{\phi}$, so that $V_{,\phi}(\phi) = V_{,\phi}(\bar{\phi} + \phi_{\mathrm{Q}}) \simeq V_{,\phi}(\bar{\phi}) + V_{,\phi\phi}(\bar{\phi})\phi_{\mathrm{Q}}$ at leading order in ϕ_{Q}.

Now let us consider the Hamiltonian (2.2.5) and introduce the coarse-grained fields with their quantum fluctuations into that expression. We can expand up to second order, meaning for example that $V(\phi) \simeq V(\bar{\phi}) + V_{,\phi}(\bar{\phi})\phi_{\mathrm{Q}} + V_{,\phi\phi}(\bar{\phi})\phi_{\mathrm{Q}}^2/2$ and keep all terms that are exactly of second order. Using expression (2.2.6), reveals that the total Hamiltonian in the scalar sector for the perturbed system is given by

$$\mathcal{C}_\phi \propto \int \mathrm{d}^3 x \left[N\left(\mathcal{C}^{(2)} + A_{\mathrm{Q}}\mathcal{C}^{(1)}\right) + \left(\partial^i B_{\mathrm{Q}}\right)\mathcal{C}_i^{(1)}\right], \tag{A.7}$$

where

$$\mathcal{C}^{(2)} = \frac{\pi_Q^2}{2a^3} + \frac{a}{2}\partial^i\phi_Q\partial_i\phi_Q + \frac{a^3}{2}V_{,\phi\phi}\phi_Q^2, \tag{A.8}$$

$$\mathcal{C}^{(1)} = \frac{1}{a^3}\bar{\pi}\pi_Q + a^3V_{,\phi}\phi_Q, \tag{A.9}$$

$$\mathcal{C}_i^{(1)} = \bar{\pi}\partial_i\phi_Q. \tag{A.10}$$

From this Hamiltonian, one can compute the Hamilton equations by making use of (2.2.7), which read

$$\dot{\phi}_k = \frac{N}{a^3}\left(\pi_k + A_k\bar{\pi}\right), \tag{A.11}$$

$$\dot{\pi}_k = -Nak^2\phi_k - Na^3A_kV_{,\phi} - Na^3V_{,\phi\phi}\phi_k - k^2\bar{\pi}B_k, \tag{A.12}$$

where we have turned to Fourier space. Keep in mind that these expressions were obtained by making use of the usual commutation relations satisfied by the annihilation and creation operator which appear inside the definition of the quantum fluctuations, which in Fourier space basically amount to stating that the only non-null commutators are the ones that involve the field ϕ_Q and its momentum π_Q (see section 2.2.2 for a more thorough explanation).

It is easy to see that the equations of motion (A.5) and (A.6) for the coarse-grained fields, in conjunction with the equations of motion (A.11) and (A.12) for the quantum fluctuations, give rise once again to (2.2.23) and (2.2.24), with quantum noises given precisely as (2.2.25) and (2.2.26). This means that the coarse-grained fields do not feel the coupling at all, and follow the same evolution as in the uncoupled case. Therefore (3.2.1) still holds even in the general case.

On the other hand, the equation of motion for ϕ_k receives an extra term, as previously claimed. Following the standard procedure, we can take the time derivative of (A.11), using (A.12) and (A.6) to make some simplifications, which takes us to the result

$$\begin{aligned}\phi_{k,N_eN_e} + (3-\epsilon)\phi_{k,N_e} + \left[\left(\frac{k}{aH}\right)^2 + \frac{V_{,\phi\phi}}{H^2}\right]\phi_k \\ - \frac{1}{a^3H^2}\left(2a^3A_kV_{,\phi} - H\bar{\pi}A_{k,N_e} + k^2H\bar{\pi}B_k\right)\phi_k = 0,\end{aligned} \tag{A.13}$$

where $,N_e$ indicates derivation with respect to number of e-foldings. At this point, one can find the gravitational constraints, which will relate A_k and B_k to ϕ_k, finally reaching the end result

$$\begin{aligned}\phi_{k,N_eN_e} + (3-\epsilon)\phi_{k,N_e} + \left\{\left(\frac{k}{aH}\right)^2 + \frac{V_{,\phi\phi}}{H^2}\right. \\ \left. - \frac{1}{M_{\rm Pl}^2a^3H}\frac{\mathrm{d}}{\mathrm{d}N}\left[a^3H\left(\frac{\mathrm{d}\bar{\phi}}{\mathrm{d}N}\right)^2\right]\right\}\phi_k = 0.\end{aligned} \tag{A.14}$$

Appendix B

A realistic potential

In this work we have made use of the potential introduced in [14] to compare our results with a realistic case. It was found in the framework of fibre inflation and type IIB flux compactifications. The name stems from the fact that the underlying Calabi-Yau compactification manifold has a particular fibre-like structure. These models show a potential of the form

$$V_{\text{inf}} = V_0(1 - e^{-n\phi/f}), \tag{B.1}$$

where ϕ is the single scalar field driving inflation called inflaton. The constants V_0, f and n depend on the particular string model one employs. This potential is of interest because it has a very flat plateau at large ϕ. However, the potential sketched in (B.1) can never generate PBHs due to its simplicity. Nonetheless, new string loop corrections suggest there might be more terms that can still be added to (B.1) in order to allow for a second plateau at small ϕ, triggering USR. These terms generally look like

$$\delta V_{\text{inf}} = -\epsilon_1 V_0 \frac{e^{2n\phi/f}}{1 + \epsilon_2 e^{3n\phi/f}}, \tag{B.2}$$

where $\epsilon_1 \ll 1$ and $\epsilon_2 \ll 1$ can be tuned to find agreement with experimental bounds. The potential (B.1) with the addition of some terms of the form (B.2) is rich enough, with some further manipulation, to allow for PBH formation at PBH scales while leaving CMB scales unscathed.

The role of the inflaton is taken by a Kähler modulus τ_{K3} controlling the size of a K3 divisor fibred over a $\mathbb{P}^1$ base with volume $t_{\mathbb{P}^1}$. The Calabi-Yau volume looks like

$$\mathcal{V} = t_{\mathbb{P}^1}\tau_{\text{K3}} - \tau_{\text{dP}}^{3/2}, \tag{B.3}$$

where τ_{dP} is the volume of a diagonal del Pezzo divisor. At leading order in the perturbative expansion $1/\mathcal{V} \ll 1$ only the directions specified by $\mathcal{V}$ and τ_{dP} are lifted, while the remaining direction, which can be parametrised by τ_{K3}, flattens. The field τ_{K3} is

a very promising inflaton candidate since it enjoys an effective non-compact rescaling symmetry.

This symmetry however has to be slightly broken to generate the correct inflationary background. This is achieved through open string 1-loops.

The potential is strikingly similar to that of Starobinsky inflation. Indeed, both models require a trans-Planckian field range to obtain enough e-foldings of inflation, leading to a promising result for the predicted tensor-to-scalar ratio $r \sim 0.005 \div 0.01$.

At leading order in $1/\mathcal{V}$, the fields $\mathcal{V}$ and τ_{dP} after stabilisation are heavier than the Hubble constant, hence play no significant role during inflation. The remaining light field τ_{K3} is left alone to drive inflation. The potential that guides this field is given by

$$
\begin{aligned}
V_{\mathrm{inf}} = \frac{W_0^2}{\mathcal{V}^2} \Bigg(& \frac{C_{\mathrm{up}}}{\mathcal{V}^{4/3}} + g_{\mathrm{s}}^2 \frac{C_{\mathrm{KK}}}{\tau_{\mathrm{K3}}^2} + \frac{W_0^2}{\sqrt{g_{\mathrm{s}}}} \frac{\epsilon_{\mathrm{F4}}}{\mathcal{V}\tau_{\mathrm{K3}}} - \frac{C_{\mathrm{W}}}{\mathcal{V}\sqrt{\tau_{\mathrm{K3}}}} \\
& + g_{\mathrm{s}}^2 D_{\mathrm{KK}} \frac{\tau_{\mathrm{K3}}}{\mathcal{V}^2} + \delta_{\mathrm{F4}} \frac{W_0^2}{\sqrt{g_{\mathrm{s}}}} \frac{\sqrt{\tau_{\mathrm{K3}}}}{\mathcal{V}^2} \Bigg).
\end{aligned}
$$

(B.4)

In this expression, all quantities but the modulus τ_{K3} are constants after tree-level stabilisation. Here $g_{\mathrm{s}} \ll 1$ is the string coupling constant and $W_0 \sim \mathcal{O}(1 \div 10)$ is the superpotential generated by background fluxes. C_{up} controls the uplifting contribution and depends on the minimum of the potential. $C_{\mathrm{KK}} > 0$, $D_{\mathrm{KK}} > 0$ and C_{W} are the coefficients of the 1-loop corrections. They are expected to be of order unity: $C_{\mathrm{KK}} \sim D_{\mathrm{KK}} \sim C_{\mathrm{W}} \sim \mathcal{O}(1)$. Finally, $\epsilon_{\mathrm{F4}} > 0$ and $\delta_{\mathrm{F4}} > 0$ only depend on specific topological properties of the underlying geometry and are expected to be relatively small: $\epsilon_{\mathrm{F4}} \sim \delta_{\mathrm{F4}} \sim \mathcal{O}(10^{-3})$.

In order to continue our analysis of this potential, it is useful to write the modulus τ_{K3} in terms of its canonically normalised counterpart ϕ as

$$
\tau_{\mathrm{K3}} = e^{\frac{2}{\sqrt{3}}\phi} = \langle \tau_{\mathrm{K3}} \rangle \, e^{\frac{2}{\sqrt{3}}\hat{\phi}},
$$

(B.5)

where we have expanded ϕ about its minimum as $\phi = \frac{\sqrt{3}}{2} \ln \langle \tau_{\mathrm{K3}} \rangle + \hat{\phi}$. With this trick, (B.4) becomes

$$
V_{\mathrm{inf}} = V_0 \left(C_1 + C_2 e^{-\frac{4}{\sqrt{3}}\hat{\phi}} + C_3 e^{-\frac{2}{\sqrt{3}}\hat{\phi}} - e^{-\frac{1}{\sqrt{3}}\hat{\phi}} + C_4 e^{\frac{2}{\sqrt{3}}\hat{\phi}} + C_5 e^{\frac{1}{\sqrt{3}}\hat{\phi}} \right).
$$

(B.6)

The new constants can be expressed in terms of the old ones as

$$
\begin{aligned}
V_0 &= \frac{C_{\mathrm{W}} W_0^2}{\gamma^{1/3} \mathcal{V}^{10/3}}, & C_1 &= \gamma^{1/3} \frac{C_{\mathrm{up}}}{C_{\mathrm{W}}}, & C_2 &= g_{\mathrm{s}}^2 \frac{C_{\mathrm{KK}}}{\gamma C_{\mathrm{W}}}, \\
C_3 &= \frac{W_0^2}{\gamma^{1/3} C_{\mathrm{W}} \sqrt{g_{\mathrm{s}}}} \frac{\epsilon_{\mathrm{F4}}}{\mathcal{V}^{1/3}}, & C_4 &= \gamma g_{\mathrm{s}}^2 \frac{D_{\mathrm{KK}}}{C_{\mathrm{W}}}, & C_5 &= \gamma C_3 \frac{\delta_{\mathrm{F4}}}{\epsilon_{\mathrm{F4}}},
\end{aligned}
$$

(B.7)

where $\gamma = \langle \tau_{K3} \rangle^{3/2} / \mathcal{V}$. Although this potential is very promising, it is not yet rich enough to generate primordial black holes since it lacks the required power spectrum enhancement. In order to achieve this, one has to consider the generalized potential which arises from relaxing a few conditions.

In the first place, the quantity C_W should be viewed as a function $C_W(\tau_{K3})$ of the Kähler modulus τ_{K3}, such that

$$C_W \quad \mapsto \quad C_W(\tau_{K3}) = C_W - \frac{A_W \sqrt{\tau_{K3}}}{\sqrt{\tau_{K3}} - B_W}, \tag{B.8}$$

where the parameters $C_W \sim \mathcal{O}(1)$ and $A_W \sim \mathcal{O}(1)$ depend on the vacuum expectation values of the complex structure moduli, while $B_W \sim \mathcal{O}(1)$ depends on some topological properties of the underlying Calabi-Yau 3-fold.

Secondly, another term in the effective action can be added if we take additional winding 1-loops. These take the form

$$\delta V_W = W_0^2 \frac{\tau_{K3}}{\mathcal{V}^4} \left(D_W - \frac{G_W}{1 + R_W \frac{\tau_{K3}^{3/2}}{\mathcal{V}}} \right). \tag{B.9}$$

Similarly, $D_W \sim \mathcal{O}(1)$ and $G_W \sim \mathcal{O}(1)$ become constants only after complex structure stabilisation, while $R_W \sim \mathcal{O}(1)$ only depends on topological features.

We will now make the assumption that our model does not feature any Kaluza-Klein loop correction, hence $C_W = D_W = 0$. Furthermore, F^4 terms are expected to be negligible since they are higher derivative terms. Our model then looks like

$$V_{\inf} = \frac{W_0^2}{\mathcal{V}^3} \left[\frac{C_{up}}{\mathcal{V}^{1/3}} - \frac{C_W}{\sqrt{\tau_{K3}}} + \frac{A_W}{\sqrt{\tau_{K3}} - B_W} + \frac{\tau_{K3}}{\mathcal{V}} \left(D_W - \frac{G_W}{1 + R_W \frac{\tau_{K3}^{3/2}}{\mathcal{V}}} \right) \right]. \tag{B.10}$$

Making use of (B.5) leads to the final result

$$V_{\inf} = V_0 \left[C_1 - e^{-\frac{1}{\sqrt{3}} \hat{\phi}} \left(1 - \frac{C_6}{1 - C_7 e^{-\frac{1}{\sqrt{3}} \hat{\phi}}} \right) + C_8 e^{\frac{2}{\sqrt{3}} \hat{\phi}} \left(1 - \frac{C_9}{1 + C_{10} e^{\sqrt{3} \hat{\phi}}} \right) \right], \tag{B.11}$$

where

$$C_6 = \frac{A_W}{C_W} \sim \mathcal{O}(1), \qquad C_7 = \frac{B_W}{\gamma^{1/3} \mathcal{V}^{1/3}} \sim \mathcal{O}(1), \qquad C_8 = \gamma \frac{D_W}{C_W} \ll 1,$$

$$C_9 = \frac{G_W}{D_W} \sim \mathcal{O}(1), \qquad C_{10} = \frac{G_W}{D_W} \sim \mathcal{O}(1) \tag{B.12}$$

The potential (B.11) is rich enough to allow for such a phase to exist provided the numerical parameter are chosen wisely.

Bibliography

[1] P. Coles and F. Lucchin, *Cosmology, the Origin and Evolution of Cosmic Structure*, 2nd Edition, Wiley & Sons, New York, 2002.

[2] D. Baumann, *Inflation*, doi:10.1142/9789814327183_0010 arXiv:0907.5424 [hep-th].

[3] Mukhanov, V. (2005). *Physical Foundations of Cosmology*. Cambridge: Cambridge University Press. doi:10.1017/CBO9780511790553

[4] P. A. R. Ade *et al.* [Planck Collaboration], Astron. Astrophys. **594** (2016) A13 doi:10.1051/0004-6361/201525830 [arXiv:1502.01589 [astro-ph.CO]].

[5] D. Baumann, *Primordial Cosmology*, PoS TASI **2017** (2018) 009, doi:10.22323/1.305.0009, [arXiv:1807.03098 [hep-th]].

[6] A. H. Guth, Phys. Rev. D **23** (1981) 347 [Adv. Ser. Astrophys. Cosmol. **3** (1987) 139], doi:10.1103/PhysRevD.23.347.

[7] A. D. Linde, Phys. Lett. **129B** (1983) 177, doi:10.1016/0370-2693(83)90837-7.

[8] A. Albrecht and P. J. Steinhardt, Phys. Rev. Lett. **48** (1982) 1220 [Adv. Ser. Astrophys. Cosmol. **3** (1987) 158], doi:10.1103/PhysRevLett.48.1220.

[9] A. D. Linde, Physics Letters B, Volume 108, Issue 6, 1982, Pages 389-393, ISSN 0370-2693, doi.org/10.1016/0370-2693(82)91219-9.

[10] J. Grain and V. Vennin, JCAP **1705** (2017) no.05, 045 doi:10.1088/1475-7516/2017/05/045 [arXiv:1703.00447 [gr-qc]].

[11] M. Biagetti, G. Franciolini, A. Kehagias and A. Riotto, JCAP **1807** (2018) no.07, 032 doi:10.1088/1475-7516/2018/07/032 [arXiv:1804.07124 [astro-ph.CO]].

[12] J. M. Ezquiaga and J. García-Bellido, JCAP **1808** (2018) 018 doi:10.1088/1475-7516/2018/08/018 [arXiv:1805.06731 [astro-ph.CO]].

[13] D. Cruces, C. Germani and T. Prokopec, arXiv:1807.09057 [gr-qc].

[14] M. Cicoli, V. A. Diaz and F. G. Pedro, JCAP **1806** (2018) no.06, 034 doi:10.1088/1475-7516/2018/06/034 [arXiv:1803.02837 [hep-th]].

[15] J. Garcia-Bellido and E. Ruiz Morales, Phys. Dark Univ. **18** (2017) 47 doi:10.1016/j.dark.2017.09.007 [arXiv:1702.03901 [astro-ph.CO]].

[16] H. Motohashi and W. Hu, Phys. Rev. D **96** (2017) no.6, 063503 doi:10.1103/PhysRevD.96.063503 [arXiv:1706.06784 [astro-ph.CO]].

[17] A. A. Starobinsky, JETP Lett. **55** (1992) 489 [Pisma Zh. Eksp. Teor. Fiz. **55** (1992) 477].

[18] K. Becker, M. Becker and J. H. Schwarz, *String theory and M-theory: A modern introduction*, INSPIRE-744404;

[19] M. Cicoli, S. Downes, B. Dutta, F. G. Pedro and A. Westphal, JCAP **1412** (2014) no.12, 030 doi:10.1088/1475-7516/2014/12/030 [arXiv:1407.1048 [hep-th]].